AD-A142 129 ADAPTIVE SPREAD SPECTRUM RECEIVER USING ACOUSTIC SURFACE WAVE TECHNOLOGY..(U) RENSSELAER POLYTECHNIC INST TROY NY DEPT OF ELECTRICAL COMPUT.. P DAS ET AL. 1/1

UNCLASSIFIED 31 MAY 84 ARO-17570.8-EL DAAG29-81-K-0066 F/G 17/2 NL

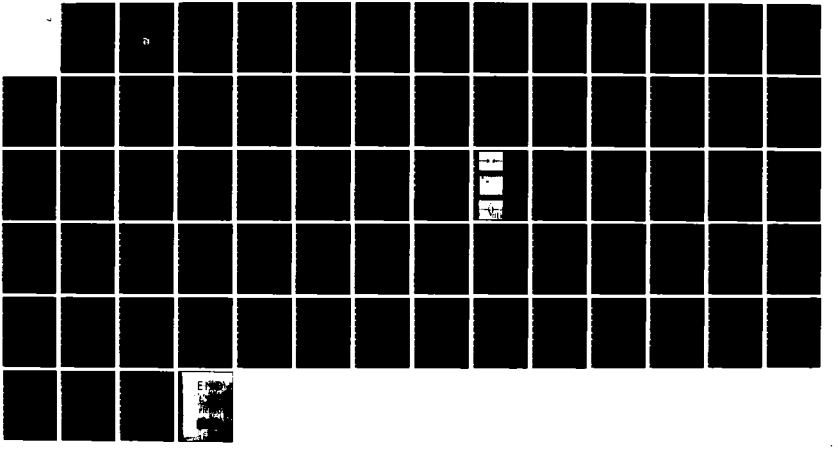

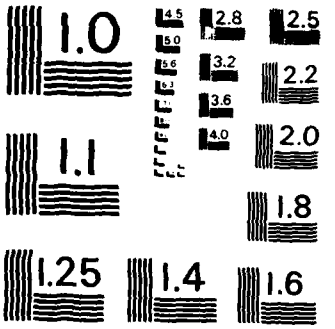

MICROCOPY RESOLUTION TEST CHART
NATIONAL BUREAU OF STANDARDS - 1963 - A

ARO 17570.8-EL

FINAL REPORT

for the contract entitled

ADAPTIVE SPREAD SPECTRUM RECEIVER USING ACOUSTIC SURFACE WAVE TECHNOLOGY

Submitted to: Army Research Office

Technical Monitor - Dr. W. Sander

ARO Contract No. DAAG 29-81-K-0066

Period Covered 4/1/81 - 3/31/84

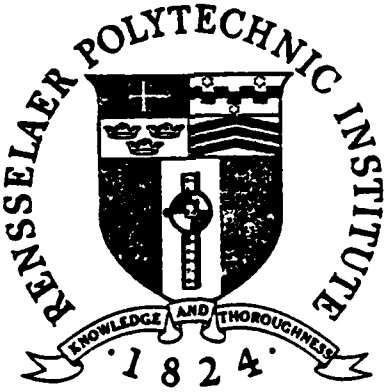

Submitted by

Prof. P. Das
Principal Investigator

Prof. L. B. Milstein
Co-Investigator

May 31, 1984

APPROVED FOR PUBLIC RELEASE;

DISTRIBUTION UNLIMITED

UNCLASSIFIED
SECURITY CLASSIFICATION OF THIS PAGE (When Data Entered)

MASTER COPY - FOR REPRODUCTION PURPOSES

REPORT DOCUMENTATION PAGE		READ INSTRUCTIONS BEFORE COMPLETING FORM
1. REPORT NUMBER ~~[illegible]~~ ARO 17570.8-EL	2. GOVT ACCESSION NO. AD-A142 119 N/A	3. RECIPIENT'S CATALOG NUMBER N/A
4. TITLE (and Subtitle) ADAPTIVE SPREAD SPECTRUM RECEIVER USING SURFACE ACOUSTIC WAVE TECHNOLOGY		5. TYPE OF REPORT & PERIOD COVERED Final Report 4/1/81 - 3/31/84
		6. PERFORMING ORG. REPORT NUMBER
7. AUTHOR(s) P. Das and L. B. Milstein		8. CONTRACT OR GRANT NUMBER(s) DAAG 29-81-K-0066
9. PERFORMING ORGANIZATION NAME AND ADDRESS Electrical, Computer, & Systems Engineering Dept. Rensselaer Polytechnic Institute Troy, New York 12180-3590		10. PROGRAM ELEMENT, PROJECT, TASK AREA & WORK UNIT NUMBERS
11. CONTROLLING OFFICE NAME AND ADDRESS U. S. Army Research Office Post Office Box 12211 Research Triangle Park, NC 27709		12. REPORT DATE May 31, 1984
		13. NUMBER OF PAGES
14. MONITORING AGENCY NAME & ADDRESS(if different from Controlling Office)		15. SECURITY CLASS. (of this report) Unclassified
		15a. DECLASSIFICATION/DOWNGRADING SCHEDULE

16. DISTRIBUTION STATEMENT (of this Report)

Approved for public release; distribution unlimited.

17. DISTRIBUTION STATEMENT (of the abstract entered in Block 20, if different from Report)

NA

18. SUPPLEMENTARY NOTES

The view, opinions, and/or findings contained in this report are those of the author(s) and should not be construed as an official Department of the Army position, policy, or decision, unless so designated by other documentation.

19. KEY WORDS (Continue on reverse side if necessary and identify by block number)

Spread spectrum, communications systems, SAW devices, adaptive systems

20. ABSTRACT (Continue on reverse side if necessary and identify by block number)

This technical report summarizes the results of the research we have been engaged in regarding the use of surface acoustic wave devices in direct sequence spread spectrum receivers. The heart of this research has been the use of the device as a real-time Fourier transformer. A system of this type is sometimes referred to as a compressive receiver, and our use of the system has been primarily as a means to implement a narrowband interference rejection filter. In addition, we have studied many other topics such as rapid acquisition, Hilbert transform generation, etc., and these topics are all overviewed in this report.

DD FORM 1 JAN 73 1473 EDITION OF 1 NOV 65 IS OBSOLETE

UNCLASSIFIED
SECURITY CLASSIFICATION OF THIS PAGE (When Data Entered)

CONTENTS

A-1

ABSTRACT

This technical report summarizes the results of the research we have been engaged in regarding the use of surface acoustic wave devices in direct sequence spread spectrum receivers. The heart of this research has been the use of the device as a real-time Fourier transformer. A system of this type is sometimes referred to as a compressive receiver, and our use of the system has been primarily as a means to implement a narrowband interference rejection filter. In addition, we have studied many other topics such as rapid acquisition, Hilbert transform generation, etc., and these topics are all overviewed in this report.

1. INTRODUCTION

During the course of this research, the main emphasis has been on narrowband interference rejection in direct sequence (SD) spread spectrum communications. The research was both analytical and experimental in nature, and comparisons between the two sets of results always indicated excellent agreement. In addition, various topics other than narrowband interference rejection were studied, and these will be summarized below. The details of these research findings have been reported in the form of papers published and papers presented in various national and international meetings. These are listed in the appendix. In this report the results are discussed briefly.

The heart of virtually all the research was the use of a surface acoustic wave (SAW) device to perform a real-time Fourier transform. The output of this Fourier transformer was then filtered by multiplying its output, in real-time, with a time waveform which represented the transfer function of an appropriate filter (e.g., a notch filter), and this product was then inverse transformed. Finally, the output of the inverse Fourier transformed was passed through a conventional DS receiver. This entire operation was referred to as transform domain processing (TDP)

For the case of narrowband interference rejection, the interference was taken to be a single tone at an arbitrary frequency with respect to the carrier frequency of the desired signal. Both experimental and analytical results were obtained for the average probability of error of the system when the interferer was fixed at a known location. Results of this type were obtained for both rectangular and cosine-shaped window functions at the input to the Fourier transformer.

In addition, it was experimentally verified that when the location of the interferer was unknown (indeed, when the frequency of the interferer was swept slowly across the band), an adaptive version of the system described above could be implemented to provide close to the same degree

of interference rejection as when the location of the interference was known exactly.

Using the same type of system, the effect of wideband Gaussian interference was analytically studied. For this case, the notch filter used to reject the narrowband interference was replaced with a prewhitening filter (i.e., a filter whose transfer functions was the inverse of the power spectral density of the noise).

As indicated above, topics other than interference rejections were also studied. The problem of rapid acquisition of the correct phase of the spreading sequence of a DS system was examined, and a new acquisition scheme using parallel SAW convolvers was proposed and analyzed. It was shown that a significant decrease in acquisition time could be achieved by using such a technique.

Finally, the use of TDP to generate waveforms other than Fourier transforms was considered, and techniques were developed to generate, in real-time, Fresnel transforms, Hilbert transforms, and single-sideband signals.

2. NARROWBAND INTERFERENCE REJECTION

Because the key result of our research is the narrowband interference rejection, in this section we will describe the operation of the system when used as a narrowband interference rejection filter and derive its performance. All the technical details of this section can be found in [1] and [2].

The receiver to be analyzed is shown in Fig. 1. The input consists of the sum of the transmitted signal $\pm s(t)$, the additive thermal noise $n(t)$ and the interference $I(t)$. The Fourier transform of the input is taken,

the transform is multiplied by the transfer function of some appropriate filter $H_c(w)$, the inverse transform of the product is taken and the resulting waveform is put through a detection filter matched to s(t).

Since the system is linear, the three components of the input can be treated separately. Denoting any of them by f(t), assumed nonzero for $t\varepsilon[0,T]$, the signal at point (1) in Fig. 1 is given by

$$f_1(t) = \int_0^T f(\tau)\cos(w_a\tau - \beta\tau^2)\cos(w_a(t-\tau) + \beta(t-\tau)^2)d\tau$$

Simplifying, this yields

$$f_1(t) = (1/2)\cos(w_a t + \beta t^2)\int_0^T f(\tau)\cos 2\beta t\tau dt$$

$$+ (1/2)\sin(w_a t + \beta t^2)\int_0^T f(\tau)\sin 2\beta t\tau dt$$

$$+ 1/2\int_0^T f(\tau)\cos(2w_a\tau - 2\beta\tau^2 + 2\beta t\tau - w_a t - \beta t^2)d\tau \qquad (1)$$

$$\simeq (1/2)F_R(2\beta t)\cos(w_a t + \beta t^2)$$

$$- (1/2)F_I(2\beta t)\sin(w_a t + \beta t^2) \qquad (2)$$

where $F_R(w)$ and $F_I(w)$ are the real and imaginary parts, respectively, of the transform of f(t), and the approximation used in going from (1) to (2) was to ignore the third term of (1) which is a double frequency term. Alternately, if it is desired to exactly cancel the third term, one can

implement the system shown in Fig. 2. Note that this requires twice as much equipment and, as a practical matter, it is usually not needed.

Having transformed f(t), it is now desired to filter it with a filter whose transfer function is $H_1(w)$. In Fig. 1 it can be seen that the output of the first chirp filter is multiplied by $H_c(2\beta t)$. This function is related to the desired transfer function $H_1(w) = H_R(w) + j\, H_I(w)$ by

$$H_c(2\beta t) = 4H_R(2\beta t) \cos 2\beta t\, T_1 + 4H_I(2\beta t) \sin 2\beta t\, T_1 \qquad (3)$$

The terms $\cos 2\beta t T_1$ and $\sin 2\beta t T_1$ shift the region the input signal is located in from $[0,T]$ to $[T_1, T_1 + T]$. This is necessary because the inverse transform filter can be shown to yield an accurate inverse transform only in the range $t\varepsilon[T_1, T_1 + T]$ (see [1]).

For our purposes, the only filters $H_1(w)$ that will be considered will be purely real, so that $H_c(2\beta t)$ will be taken to be

$$H_c(2\beta t) = 4H_R(2\beta t) \cos 2\beta t T_1$$

resulting in a waveform at point (2) of Fig. 1 given by

$$f_2(2\beta t) = H_R(2\beta t)\, \{F_R(2\beta t) \cos[(w_a - 2\beta T_1)t + \beta t^2] - F_I(2\beta t) \sin[(w_a - 2\beta T_1)t + \beta t^2]\} \qquad (4)$$

assuming the sum frequency terms at $w_a + 2\beta T_1$ are filtered out.

It was shown in [1] that the region in frequency where the transform is accurate is the range $\omega\varepsilon[2\beta T, 2\beta T_1]$. Therefore, limiting the input to the inverse transform chirp filter to $t\varepsilon[T, T_1]$ yields a waveform at point (3) of Fig. 1 described by

$$f_3(2\beta t) = \int_T^{T_1} \Big\{ H_R(2\beta\tau) F_R(2\beta\tau) \cos(w_r\tau + \beta\tau^2)$$

$$- H_R(2\beta\tau) F_I(2\beta\tau) \sin(w_r\tau + \beta\tau^2)$$

$$\cdot \cos[w_a(t - \tau) - (t^2 - 2t\tau + \tau^2)]d\tau \Big\} \qquad (5)$$

where $w_r \triangleq w_a - 2\beta T_1$.

Expanding the terms in (5) and noting that the only term of interest for a real function f(t) is the term modulating $\cos(w_a t - \beta t^2)$, the output of the lowpass filter at point (4) of Fig. 1 is given by

$$f_4(t) = \int_T^{T_1} H_R(2\beta\tau)[F_R(2\beta\tau) \cos(2\beta(t - T_1)\tau)$$

$$- F_I(2\beta\tau) \sin(2\beta(t - T_1)\tau)]d\tau \qquad (6)$$

Finally, the output of the matched filter at point (5) is given by

$$f_0(T_1 + T) = \int_{T_1}^{T_1+T} f_4(t)s(t - T_1)dt$$

$$= \int_0^T \int_T^{T_1} s(t) \left\{ H_R(2\beta\tau) \left[\int_0^T f(\lambda) \cos 2\beta\tau\lambda d\lambda \right] \cos 2\beta t\tau \right.$$

$$\left. + H_R(2\beta\tau) \left[\int_0^T f(\lambda) \sin 2\beta\tau\lambda d\lambda \right] \sin 2\beta t\tau \right\} d\tau dt \qquad (7)$$

Letting $w = 2\beta\tau$ and interchanging the order of integrations yields (to within the constant factor 2β)

$$f_0(T_1 + T) = \int_0^T \int_{2\beta T}^{2\beta T_1} \int_0^T s(t) \, [H_R(w)f(\lambda) \cos w\lambda \cos wt$$

$$+ H_R(w)f(\lambda) \sin w\lambda \sin wt]d\lambda dw dt$$

$$= \int_0^T f(\lambda) \left\{ \int_{2\beta T}^{2\beta T_1} H_R(w) \left[\int_0^T s(t)(\cos wt \cos w\lambda + \sin wt \sin w\lambda)dt \right] dw \right\} d\lambda$$

$$= \int_0^T f(\lambda) \left\{ \int_{2\beta T}^{2\beta T_1} H_R(w) \, [S_R(w) \cos w\lambda - S_I(w) \sin w\lambda] \, dw \right\} d\lambda \qquad (8)$$

where $S_R(w) + j\, S_I(w)$ is the Fourier transform of $s(t)$. Assuming that $H_R(w)$ is bandlimited to $w \in [2\beta T, 2\beta T_1]$ or less yields (to within a constant factor)

$$f_0(T_1 + T) = \int_0^T f(\lambda) \mathcal{F}^{-1} \{H_R(w)S(w)\} d\lambda$$

$$= \int_0^T f(\lambda) \, [h_R(\lambda) * s(\lambda)] d\lambda \qquad (9a)$$

where $h_R(t) \triangleq \mathcal{F}^{-1} (H_R(w))$.

The assumption that $H_R(w)$ is zero outside of $w \in [2\beta T, 2\beta T_1]$ is not restrictive, given the fact that the original transform was accurate only in that range. However, the significance of the assumption is as follows: The system output as given by (9a) can be shown to equal

$$\int_0^T s(t)[f(t) * h_R(t)]dt \qquad (9b)$$

This can be seen by noting that (9b) is just the output of a filter matched to $f(t) * h_R(t)$ when $s(t)$ is the input and when the filter is sampled at $t = T$. Consequently,

$$\int_0^T s(t)[f(t) * h_R(t)]dt = \frac{1}{2\pi}\int_{-\infty}^{\infty} S(w)F^*(w)H_R(w)e^{-jwT}e^{jwt}dw\Big|_{t=T}$$

$$= \frac{1}{2\pi}\int_{-\infty}^{\infty} S(w)F^*(w)H_R(w)dw$$

Using the same reasoning, (9a) can be shown to equal

$$\frac{1}{2\pi}\int_{-\infty}^{\infty} F(w)S^*(w)H_R(w)dw$$

and so (9a) and (9b) are complex conjugates. (Recall from (3) that $H_R(w$ is real.) Since they are both real, they are clearly equal. Since (9b) ... the output of a conventional system (i.e., one in which the filtering i... performed directly in the "time domain"), it is seen that the system of Figure 1 will perform very closely to whatever particular conventional system it is trying to emulate. Note that even if the transforms were exact, the two systems would not perform identically the same, because the above analysis assumes a time-limited input, and while this is a reasonable assumption for the signal component of the received waveform, the noise in most conventional systems is assumed to exist for all time. Also, note that intersymbol interference has been neglected. This was done neither as an approximation nor as an oversight. As described in [1], to process a contiguous-time data stream, finite segments of the incoming waveform have to be time gated and processed separately. If this time gating is performed one symbol at a time, adjacent symbols can be received without interfering with one another. The key difference between the two systems, however, is the fact that components such as ideal rectangular filters cannot be implemented in a conventional sense, but using the transform

technique, filtering with an ideal bandlimited filter corresponds simply to multiplying the transform output with an appropriate timing gate. Finally, it can now clearly be seen how large the range $w\varepsilon[2\beta T, 2\beta T_1]$ has to be relative to a given signal and interference combination, since whatever bandwidth one would want for $H_R(w)$ in a conventional system is the range of frequencies $[2\beta T, 2\beta T_1]$ for which one wants the Fourier transform of Fig. 1 to be valid.

To use (9b) to determine the performance of a wideband system being interfered with by a narrowband signal (e.g., a jammer), assume the transmitted signal is a binary waveform where each information-bearing symbol has superimposed upon it the seven-bit, pseudo-noise (PN) sequence - 1 - 1 - 1 11 - 1 1, with T_c the duration of each PN code chip. The noise n(t) is additive white Gaussian noise (AWGN) with two-sided spectral density $(\eta_0/2)$ and the interference I(t) is the tone $\alpha\cos[(w_0 + \delta w_0)\ t + \theta]$ where α is constant, w_0 is the carrier frequency of the transmitted signal, and θ is a random phase uniformly distributed between 0 and 2π.

Each symbol is assumed to be detected independently of other symbols. Hence the input to the forward Fourier transformer of Fig. 1, while certainly not time-limited to [0,T], can be considered to be observed in disjoint T-second intervals. Therefore the input to the system for any given symbol is effectively described by the sum of that T-second long pulse plus a T-second segment of both the additive noise and the interfering signal. With this model, the output statistic $g(T_1 + T)$ equals (from (9a))

$$g(T_1 + T) = \int_0^T [\pm s(t) + n(t) + I(t)][h_R(t) * s(t)]dt \qquad (10)$$

Denoting the signal, noise, and interference terms in (10) by S_0,n_0, and I_0 respectively, the noise term n_0 is clearly a Gaussian random variable with mean and variance given by

$$E(n_0) = 0 \tag{11}$$

and

$$\sigma_{n_0}^2 = (\eta_0/2) \int_0^T [h_R(t) * s(t)]^2 \, dt \tag{12}$$

respectively, and the average probability of error of the system, assuming equally likely symbols, is given by

$$P_e = \frac{1}{2\pi} \int_0^{2\pi} \Phi \left(- \frac{S_0 + I_0}{\sigma_{n_0}} \right) d\theta \tag{13}$$

where

$$\Phi(x) \triangleq \frac{1}{\sqrt{2\pi}} \int_{-\infty}^{x} e^{-y^2/2} \, dy$$

and where I_0 is an explicit function of θ.

To compute either the noise variance or either of the deterministic terms in (10), one needs to specify a filter $h_R(t)$ and compute

$$s(t) * h_R(t) = F^{-1} \{S(w)H_R(w)\} \, . \tag{14}$$

For a bandpass notch filter with upper cutoff $w_0 + \Delta w > w_0 + \delta w_0$ and a notch of width $2\delta w$ at $w_0 + \delta w_0$, the filter transfer function is given by

$$H_R(w) = P_{\delta w}(w - w_0) - P_{\delta w}(w - w_0 - \delta w_0) + P_{\delta w}(w + w_0) - P_{\delta w}(w + w_0 + \delta w_0) \tag{15}$$

For the seven-bit PN sequence input signal described above, it is easily shown that its Fourier transform $S_i(w)$ is given by

$$S_i(w) = \frac{-2\sin 3wT_c + 2\sin 5wT_c - 2\sin 6wT_c + \sin 7wT_c}{w}$$

$$+ j\,\frac{1 - 2\cos 3wT_c + 2\cos 5wT_c - 2\cos 6wT_c + \cos 7wT_c}{w} \qquad (16)$$

Expressing $s(t)$ as $s_i(t)\cos w_0 t$, where $s_i(t) = \mathcal{F}^{-1}\{S_i(w)\}$ it can be shown that

$$s(t) * h_R(t) = [R_1(t;\Delta w) - (1/2)\,R_2(t)]\cos w_0 t - (1/2)\,R_3(t)\sin w_0 t \qquad (17)$$

where

$$R_1(t;\Delta w) = -\frac{1}{\pi}\{\mathrm{Si}\,\Delta wt - 2\,\mathrm{Si}\,\Delta w(t - 3T_c) + 2\,\mathrm{Si}\,\Delta w(t - 5T_c)$$

$$- 2\,\mathrm{Si}\,\Delta w(t - 6T_c) + \mathrm{Si}\,\Delta w(t - 7T_c)\}\,, \qquad (18)$$

$$R_2(t) \triangleq -(1/\pi)\{\mathrm{Si}(\delta w_0+\delta w)t - \mathrm{Si}(\delta w_0 - w)t - 2[\mathrm{Si}(\delta w_0+\delta w)(t-3T_c) - \mathrm{Si}(\delta w_0-\delta w)(t-3T_c)]$$
$$+ 2[\mathrm{Si}[(\delta w_0+\delta w)(t-5T_c)] - \mathrm{Si}(\delta w_0-\delta w)(t-5T_c)]$$
$$- 2[\mathrm{Si}(\delta w_0+\delta w)(t-6T_c) - \mathrm{Si}(\delta w_0-\delta w)(t-6T_c)]$$
$$+ [\mathrm{Si}(\delta w_0+\delta w)(t-7T_c) - \mathrm{Si}(\delta w_0-\delta w)(t-7T_c)]\} \qquad (19)$$

and

$$R_3(t) \triangleq -(1/\pi)\{\mathrm{Ci}(\delta w_0+\delta w)t - \mathrm{Ci}(\delta w_0-\delta w)t - 2[\mathrm{Ci}(\delta w_0+\delta w)(t-3T_c) - \mathrm{Ci}(\delta w_0-\delta w)(t-3T_c)]$$
$$+ 2[\mathrm{Ci}(\delta w_0+\delta w)(t-5T_c) - \mathrm{Ci}(\delta w_0-\delta w)(t-5T_c)]$$
$$- 2[\mathrm{Ci}(\delta w_0+\delta w)(t-6T_c) - \mathrm{Ci}(\delta w_0-\delta w)(t-6T_c)]$$
$$+ [\mathrm{Ci}(\delta w_0+\delta w)(t-7T_c) - \mathrm{Ci}(\delta w_0-\delta w)(t-7T_c)]\} \qquad (20)$$

In (18), (19) and (20),

$$\mathrm{Si}(x) \triangleq \int_0^x \frac{\sin y}{y}\,dy$$

and

$$\mathrm{Ci}(x) \triangleq -\int_x^\infty \frac{\cos y}{y}\,dy\,.$$

Also, for negative x, the Cauchy principal value of Ci(x) is used.

Finally, the output of the final matched filter can be written (neglecting double frequency terms)

$$g(T_1+T) = \int_0^T [(1/2)\ s_i(t) + (\alpha/2)\cos(\delta w_0 t+\theta)+n(t)\cos\ w_o t][R_1(t;\Delta w)-(1/2)R_2(t)]dt$$

$$+ \frac{1}{2}\int_0^T [\frac{\alpha}{2}\ \sin(\delta w_0 t+\theta)-n(t)\sin\ w_o t]R_3(t)dt \qquad (21)$$

Most of the terms in (21) due to the signal and the interference, and most of the terms comprising the variance of the noise term in (21), can be evaluated in closed-form using the integral relations of ([3] p. 633]). However, the resulting expressions are exceedingly lengthy and consequently the probability of error as given by (13) will be presented numerically below. As a perspective on these results, if the received waveform described above is detected with just a filter matched to the transmitted signal s(t) (i.e., if no attempt is made to remove the interference), the average probability of error of the system will be given by

$$P_{e_{MF}} = \frac{1}{2\pi}\int_0^{2\pi} \phi\left(-\sqrt{\frac{2E}{\eta_0}} - \sqrt{\frac{2}{\eta_0 E}}\ I(T)\right)\ d\theta \qquad (22)$$

where E is the energy per bit of the transmitted signal and

$$I(T) = (\alpha/2)\int_0^T s_i(t)\ \cos(\delta w_0 t + \theta)dt$$

$$= \sqrt{\frac{2E}{T}}\ \frac{\alpha/2}{\delta w_0}\ \{[-2\ \sin 3\delta w_0 T_c + 2\ \sin 5\delta w_0 T_c - 2\ \sin 6\delta w_0 T_c + \sin 7\delta w_0 T_c]\cos\ \theta$$

$$+ [1 - 2\ \cos 3\delta w_0 T_c + 2\ \cos 5\delta w_0 T_c - 2\ \cos 6\delta w_0 T_c + \cos 7\delta w_0 T_c]\sin\ \theta\} \qquad (23)$$

There is one aspect of this model which requires elaboration, namely, the reason for the low number of chips-per-bit (i.e., the small processing gain) of the system. A short PN sequence was used because the shorter the sequence, the more pessimistic the results will be. This follows because the system shown in Fig. I only "looks" at the interferer for T seconds, so that the tone jammer actually has a spectrum whose main lobe bandwidth is 2/T. Since the way this system operates is to, for example, notch out the main lobe of the jammer, and hence unavoidably null out any signal energy in that bandwidth as well, the larger the ratio of T/T_c, the smaller is the percentage of signal power which is lost. In other words, using a very short PN sequence is essentially a worst case analysis when comparing the present system to a conventional spread spectrum system.

The results of evaluating the probability of error expressions are shown in Fig. 3. There are eight curves labelled a to d and a' to d', and Table I identifies each of those curves. The notation $P_e(\alpha = x)$ means Eq. (13) evaluated for $\alpha = x$. For these curves, the upper cutoff was always taken to be 14 π/T (corresponding to the chip rate of the PN sequence) and the notch itself was always centered at the interferer frequency and had a width of $\pm 2\pi/2T$.

Comparing the curves, one sees that the notch filter system almost always outperforms the conventional matched filter. The one exception is when the interferer's effect is initially not very significant (e.g., α near zero). This is because the signal degradation, due to the bandlimiting, is more harmful than the degradation due to the interferer. Clearly, the performance of the system using the notch filter could be further improved simply by increasing its bandwidth. The key point is that for a strong enough tone interferer, the notch filter in cascade with the matched filter will always improve the system performance.

TABLE I

INTERFERENCE LEVELS USED IN SYSTEM EVALUATION

Curve	Description
a	$P_e(\alpha = 0)$ (i.e., no interferer)
b	$P_e(\alpha = 2)$
c	$P_e(\alpha = 4)$
d	$P_e(\alpha = 8)$
a'	$P_{e_{MF}}(\alpha = 0)$
b'	$P_{e_{MF}}(\alpha = 2)$
c'	$P_{e_{MF}}(\alpha = 4)$
d'	$P_{e_{MF}}(\alpha = 8)$

Finally, it is possible to implement an adaptive version of this system as described in [2] and illustrated in Fig. 4. Its operation can be seen as follows: The upper branch envelope detects the Fourier transformed input and the output of the envelope detector is fed into a switch controlled by a threshold device. The lower branch passes the Fourier transformed input directly to the first multiplier. The switch on the upper branch is set so that any time the output of the envelope detector exceeds a predetermined level, the output of the switch is forced to zero. In this manner, the adaptive notch switch is implemented.

Notice that the remaining processing as shown on Fig. 4 is somewhat different from that shown on Fig. 1, since with the system as implemented in Fig. 4, the matched filtering is accomplished by Fourier transforming a reference signal $s(-t)$, multiplying this transform with the output of the first multiplier, and then inverse transforming the output of the second multiplier. If the two systems are compared, it will be seen that they are equivalent in the sense that they perform the same when operated under similar conditions (i.e., either both in a non-adaptive mode or both in an adaptive mode).

3. CONCLUSION

This report was meant to summarize the results we obtained regarding the use of SAW devices in DS spread spectrum communication systems. While many different topics were studied during the course of the research, the most important result was the use of the SAW devices as a real-time Fourier transformer (sometimes referred to as a compressive receiver) to implement narrowband interference rejection filters, and some of these results were summarized in the previous section.

With respect to results that we obtained on the other topics listed in the Introduction, a complete bibliography of all the publications resulting from this research is included in Appendix A. Hence the interested reader can find the details to any of our research results in one or more of the referenced papers. The following two papers have not yet been published and thus for convenience the copies of these papers are included as Appendix C and D.

> Laurence B. Milstein, John Gevargiz and Pankaj K. Das, "Rapid Acquisition for Direct Sequence Spread Spectrum Communications Using Parallel SAW Convolvers".
>
> John Gevargiz, Michael Rosenmann, P. Das and L. B. Milstein, "A Comparison of Weighted and Non-Weighted Transform Domain Processing Systems for Narrowband Interference Excision".

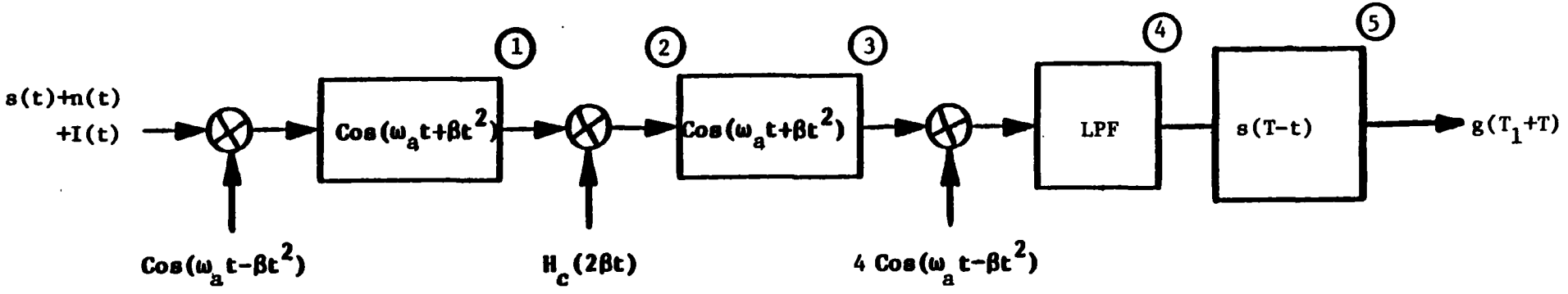

Figure 1. Transform Domain Filtering Receiver

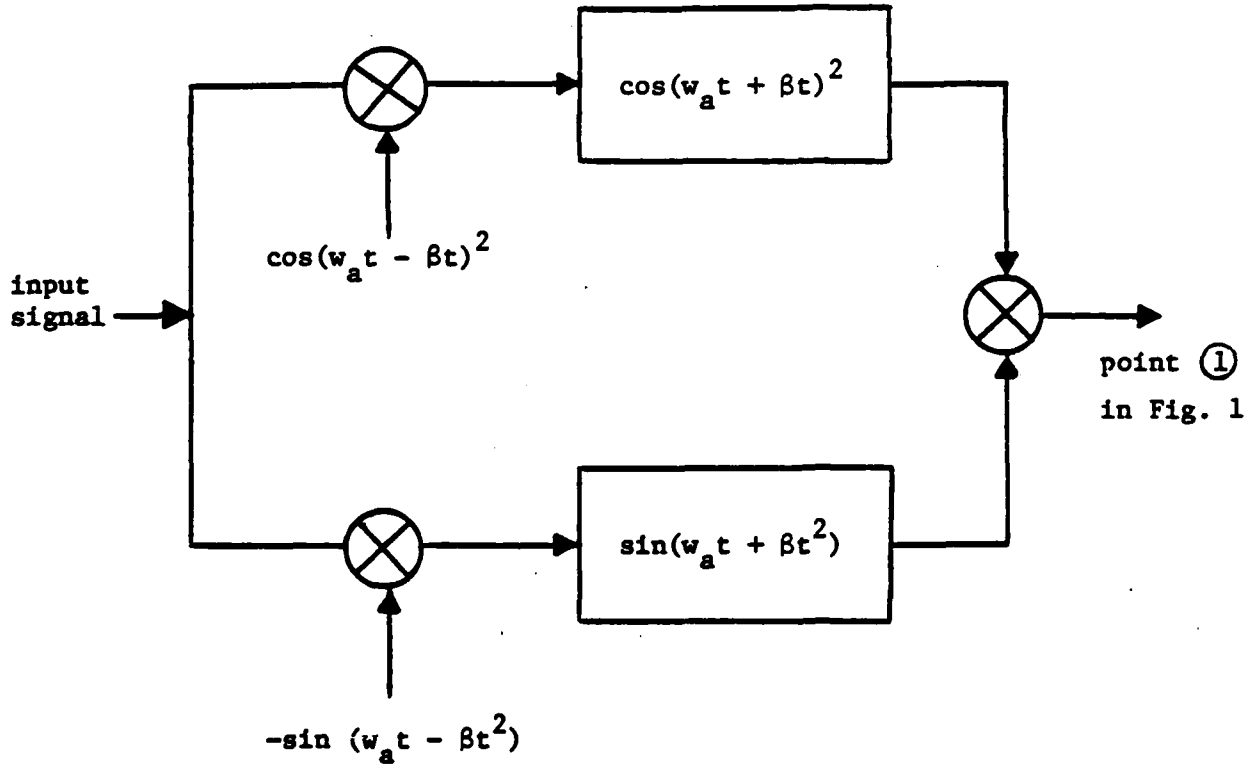

Figure 2. Exact Cancellation of Double Frequency Term

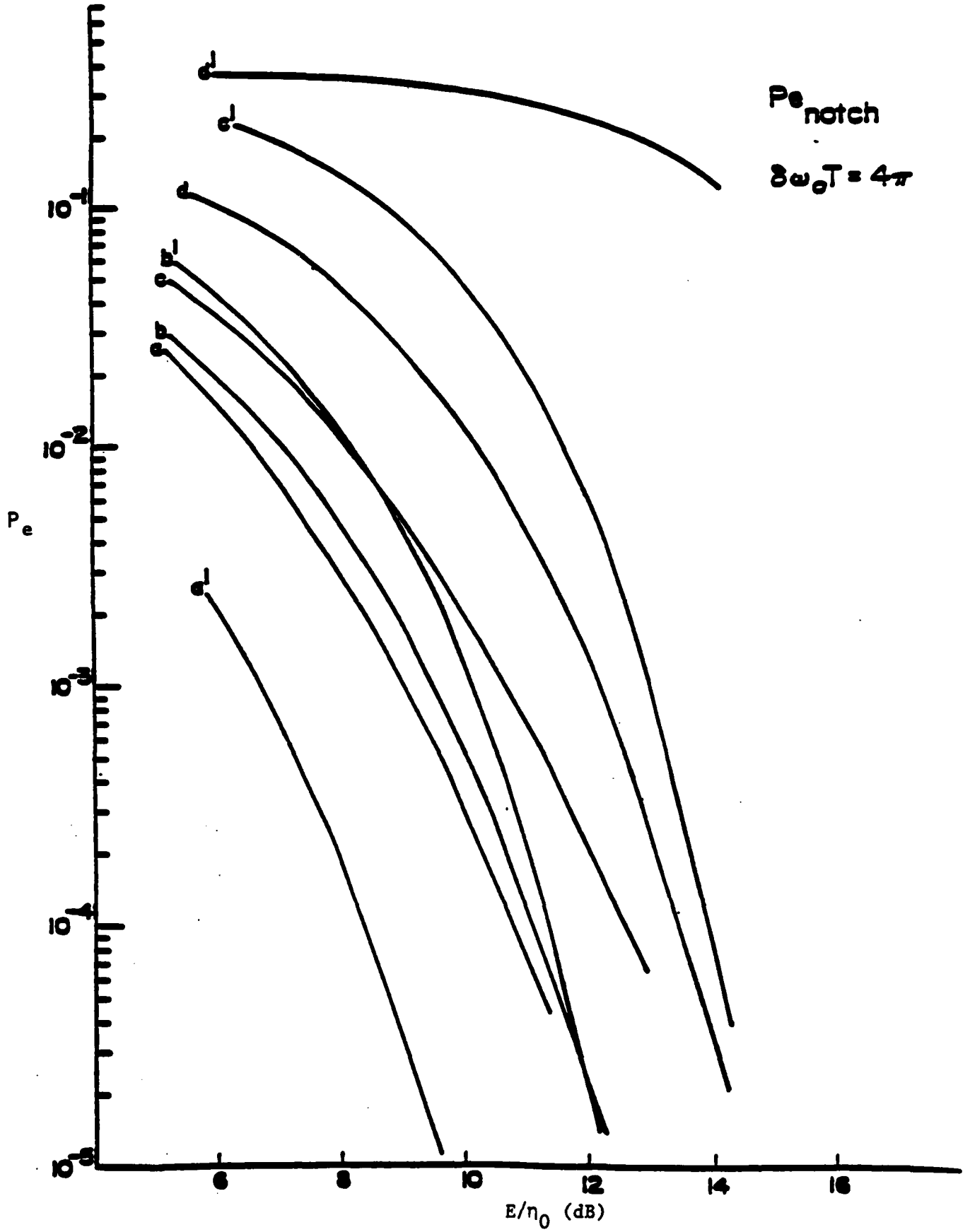

Figure 3. P_e versus E/η_0 (Match Filter)

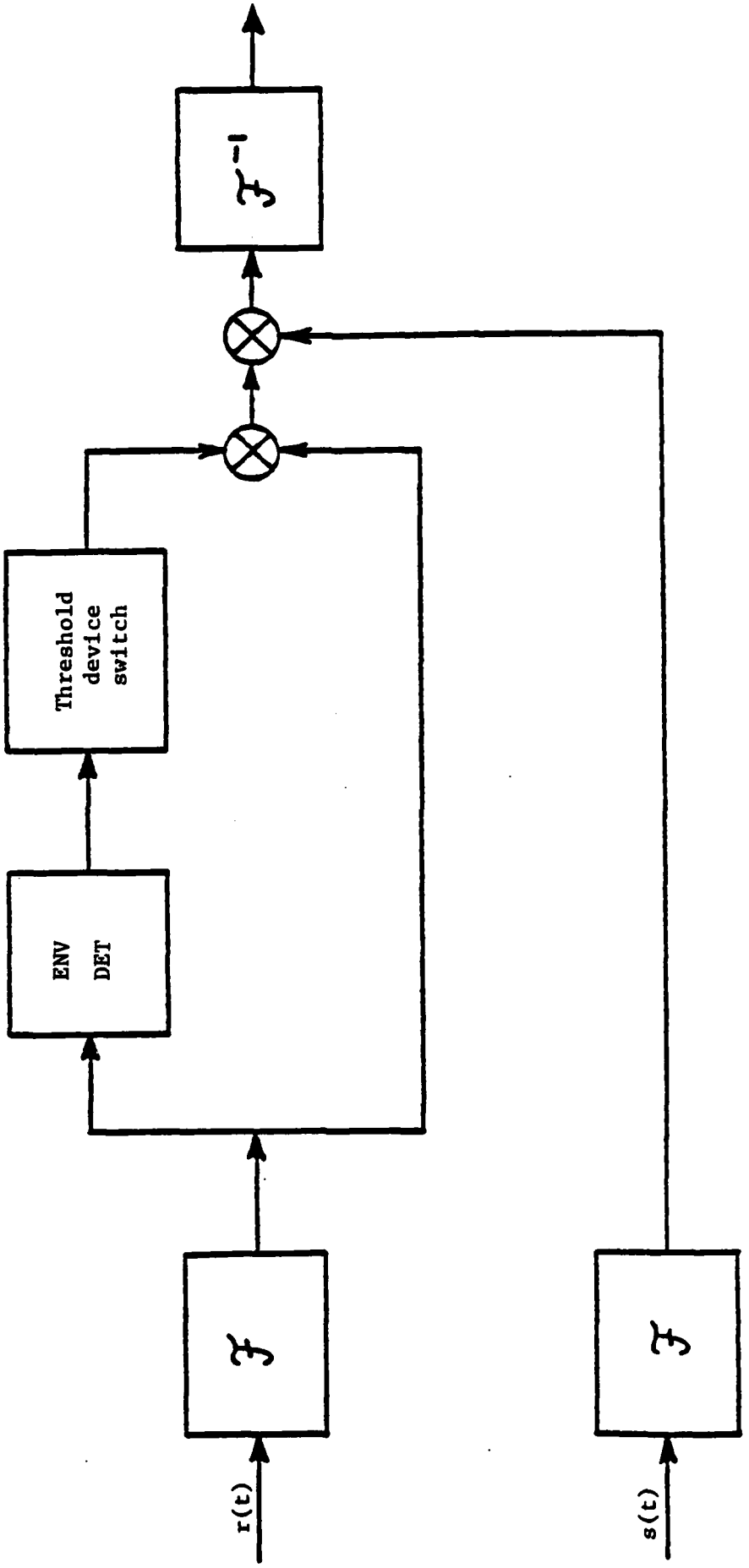

Figure 4. Adaptive Notch Filter

REFERENCES

[1] L. B. Milstein and P. K. Das, "An Analysis of a Real-Time Transfer Domain Filtering Digital Communication System - Part I: Narrowband Interference Rejection," IEEE Trans. Comm., Vol. COM-28, pp. 816-824, June 1980.

[2] D. Shklarsky, P. Das and L. B. Milstein, "Adaptive Narrowband Interference Suppression," Nat. Telecomm. Conf. Rec., Nov. 1979, pp. 15.2.1-15.2-4.

[3] I. S. Gradshteyn and I. M. Ryzhik, Tables of Integrals, Series and Products. New York: Academic, 1915.

PERSONNEL SUPPORTED BY THIS GRANT:

RPI Students

1. M. Rosenmann - (partial support) - Research Associate.

2. J. Gevargiz - (partial support) - finished M.S. in 1983 entitled "Signal Processing Using Surface Acoustic Wave Devices in a Direct Sequence Spread Spectrum Communication System".

3. D. Shklarsky - (partial support) - Research Associate.

UCSD Student

1. Charles Cobleigh - (partial support) - Research Associate

APPENDIX

A. List of papers published and to be published under the auspices of this grant*

1. P. Das, L. B. Milstein and D. R. Arsenault, "Adaptive Spread Spectrum Receiver using SAW Technology", National Telecommunication Conference Record, IEEE Publication No. 77 CH 1202-2, pp. 35.7-1-35.7-6, 1977.

2. P. Das and D. R. Arsenault, "SAW Fresnel Transform Devices and Their Applications", IEEE Ultrasonics Symposium Proceedings, IEEE Publication No. 77 CH 1264-1SU, pp. 969-973, 1977.

3. L. B. Milstein, D. R. Arsenault and P. Das, "Transform Domain Processing for Digital Communications Systems using Surface Acoustic Wave Devices", AGARD-NATO Conference Proceedings on Digital Communications, CP-239, 28-1-28-16, 1978.

4. D. R. Arsenault, P. Das and L. B. Milstein, "Matched Filtering of Continuous Signals by the Product of Transforms Technique using SAW Chirp Filters", IEEE Ultrasonics Symposium Proceedings, IEEE Publication No. 78 CH 1355-1SU, pp. 543-548, 1978.

5. L. B. Milstein, P. Das and D. R. Arsenault, "Narrowband Jammer Suppression in Spread Spectrum System using SAW Devices", National Telecommunication Conference Record, IEEE Catalog No. 78 CH 1354-OCSCB, pp. 43.2.1-3.2.5, 1978.

6. L. B. Milstein, D. R. Arsenault and P. Das, "Signal Processing with SAW Devices", International Telemetering Conference Proceedings, Vol. 16, pp. 1037-1040, 1978.

7. P. Das, L. B. Milstein and D. R. Arsenault, "Variable Format Radar Receiver using a SAW Convolver", IEEE Transactions on Aerospace and Electronic Systems, Vol. AES-14, pp. 843-852, 1978.

8. L. B. Milstein and P. Das, "An Analysis of a Real-Time Transform Domain Filtering Digital Communications System Part I: Narrowband Interference Rejection", IEEE Trans. Comm. Technology, Vol. COM-28, pp. 816-824, 1980.

9. L. B. Milstein and P. Das, "Performance Analysis of a Spread Spectrum Receiver using Transform Domain Filtering", Proceedings of the AFOSR Workshop in Communication Theory and Application, IEEE Library No. ENO 139-6, pp. 92-94.

10. P. Das, D. Shklarsky and L. B. Milstein, "SAW Implemented Real-Time Hilbert Transform and its Application in SSB", 1979 Ultrasonics Symposium Proceedings, IEEE Publication No. 79 CH 1482-9, pp. 752-756.

*This list includes publications under ARO Grant No. DAAG-29-77-G-0205 and Contract No. DAAG-20-79-C-0192.

11. D. Shklarsky, P. Das and Laurence B. Milstein, "Adaptive Narrowband Interference Suppression", Proceedings of National Telecommunication Conference, IEEE Publication No. 79 CH 1514-9, pp. 14.2.1-15.2.4.

12. P. Das, D. Shklarsky and L. B. Milstein, "The Use of the Hilbert Transform to Double the Information Rate of a SAW Implemented Direct Sequence Spread Spectrum System", Proceedings of the National Telecommunication Conference, IEEE Publication No. 80 CH 1539-6, pp. 61.4.1-61.4.5, 1980.

13. D. Shklarsky, P. Das and L. B. Milstein, "The Use of the Hilbert Transform to Double the Information Rate of a Spread Spectrum Communication System", IEEE Trans. on Vehicular Technology, Vol. VT-30, No. 1, Feb., 1981.

14. D. Shklarsky, P. Das and L. B. Milstein, "Doppler Insensitive Time Integrating Correlator Using SAW Convolver and CCD", 1980 Ultrasonics Symposium Proceedings, IEEE Cat. No. 80 CH 1602-2, pp. 10-13, 1980.

15. D. Shklarsky, P. Das and L. B. Milstein, "A SAW Filter for SSB Waveform Generation", IEEE Trans. Circuits and Systems, Vol. CAS-27, pp. 464-468, 1980.

16. D. Shklarsky, P. Das and L. B. Milstein, "Power Spectral Estimation Using SAW Convolver and Chirp Transform", 1981 Ultrasonics Symposium Proceedings, IEEE Catalog No. 81-CH-1689-9, pp. 252-255, 1981.

17. L. B. Milstein and P. Das, "A SAW Implemented Wideband Interference Rejection Spread Spectrum System", 1982 ICC (International Conf. on Communications), IEEE Cat. No. 1766-5, Vol. 3, pps. 7E.5.1-7E.5.5.

18. L. B. Milstein and P. Das, "An Analysis of Real-Time Transform Domain Filtering Digital Communications System - Part II: Wideband Interference Rejection", IEEE Trans. on Communication Technology, Vol. COM-31, pp. 21-27, 1983.

19. L. B. Milstein, P. Das and John Gevargiz, "Processing Gain Advantage of Transform Domain Filtering DS-Spread Spectrum Systems", Proceedings of the IEEE Military Communications Conference, IEEE Cat. #82CH 1734-3, pp. 21.2-1 to 21.2-4, 1982.

20. Laurence B. Milstein, John Gevargiz and Pankaj K. Das, "A Rapid Acquisition Technique Employing Parallel SAW Processing", Proceedings of the 1983 Military Communications Conference, IEEE Publication No. 84-CH 1909-1, pp. 501-505, 1983.

21. Michael Rosenmann, John Gevargiz, Pankaj K. Das, and Laurence B. Milstein, Probability of Error Measurement for an Interference Resistant Transform Domain Processing Receiver, Proceedings of the 1983 Military Communications Conference, IEEE Publication No. 84-CH 1909-1, pp. 636-640, 1983.

22. Laurence B. Milstein, John Gevargiz and Pankaj K. Das, "Rapid Acquisition for Direct Sequence Spread Spectrum Communications Using Parallel SAW Convolvers", to be published. (Included in this report as Appendix C).

23. John Gevargiz, Michael Rosenmann, P. Das and L. B. Milstein, "A Comparison of Weighted and Non-Weighted Transform Domain Processing Systems for Narrowband Interference Excision", to be published. (Included in this report as Appendix D).

B. List of papers presented in national and international meetings*

1. D. R. Arsenault and P. Das, "SAW Fresnel Transform Devices and Their Applications", presented at the 1977 IEEE Ultrasonics Symposium, Phoenix, Arizona, October 1977.

2. P. Das, L. B. Milstein and D. R. Arsenault, "Adaptive Spread Spectrum Receiver using SAW Technology", presented at the National Telecommunication Conference, December 5-8, 1977, Los Angeles, California.

3. L. B. Milstein, D. R. Arsenault and P. Das, "Transform Domain Processing for Digital Communications Systems using Surface Acoustic Wave Devices", Presented at the AGARD-NATO Conference on Digital Communications, Munich, Germany, June 5-9, 1978.

4. D. R. Arsenault, P. Das and L. B. Milstein, "Matched Filtering of Continuous Signals by the Product of Transforms Technique using SAW Chirp Filters", presented at the 1978 Ultrasonics Symposium held at Cherry Hill, NJ, September 25-27, 1978.

5. L. B. Milstein and P. Das, "Performance Analysis of a Spread Spectrum Receiver using Transform Domain Filtering", presented at the AFOSR Workshop in Communication Theory and Applications, held September 18-20, 1978, Provincetown, Massachusetts.

6. L. B. Milstein, D. R. Arsenault and P. Das, "Signal Processing with SAW Devices", presented at the International Telemetering Conference, Los Angeles, Nov. 14-16, 1978.

7. L. B. Milstein, D. R. Arsenault and P. Das, "Signal Processing with SAW Devices", presented at the International Telemetering Conference, Los Angeles, Nov. 14-16, 1978.

8. P. Das, D. Shklarsky and L. B. Milstein, "SAW-Implemented Real-Time Hilbert Transform and its Applications in SSB", presented at the Ultrasonics Symposium, New Orleans, Sept. 26-29, 1979.

9. D. Shklarsky, P. Das and L. B. Milstein, "Adaptive Narrowband Interference Suppression", presented at the National Telecommunications Conference, Washington, D.C., November 27-29, 1979.

*This list includes presentations under ARO Grant No. DAAG-29-77-G-0205 and Contract No. DAAG-20-79-C-0192.

10. P. Das, D. Shklarsky and L. B. Milstein, "The Use of the Hilbert Transform to Double the Information Rate of a SAW Implemented Direct Sequence Spread Spectrum System", presented at the National Telecommunication Conference, Houston, Texas, Dec. 1-4, 1980.

11. D. Shklarsky, P. Das and L. B. Milstein, "Doppler Insensitive Time Integrating Correlator using SAW Convolver and CCD", presented at the Ultrasonics Symposium, Boston, Massachusetts, Nov. 5-7, 1980.

12. Dan Shklarsky, P. Das and L. B. Milstein, "Power Spectrum Estimation Using SAW Convolver and Chirp Transform", presented at the IEEE Ultrasonics Symposium, Chicago, Illinois, October 14-16, 1981.

13. Laurence B. Milstein and P. Das, "A SAW Implemented Wideband Interference Rejection Spread Spectrum System", presented at the ICC (international Conference on Communications), Philadelphia, June 14-17, 1982.

14. Laurence B. Milstein, Pankaj K. Das and John Gevargiz, "Processing Gain Advantage of Transform Domain Filtering DS-Spread Spectrum Systems", presented at the IEEE Military Communications Conference, Boston, MA, October 17-20, 1982.

15. Laurence B. Milstein, John Gevargiz and Pankaj K. Das, "A Rapid Acquisition Technique Employing Parallel SAW Processing", presented at MILCOM '83, Washington, D.C., October 31 - November 2, 1983.

16. Michael Rosenmann, John Gevargiz, Pankaj K. Das and Laurence B. Milstein, "Probability of Error Measurement for an Interference Resistant Transform Domain Processing Receiver", presented at MILCOM '83, Washington, D.C., October 31 - November 2, 1983.

APPENDIX C

A COMPARISON OF WEIGHTED AND NON-WEIGHTED TRANSFORM DOMAIN PROCESSING SYSTEMS FOR NARROWBAND INTERFERENCE EXCISION*

by

John Gevargiz, Michael Rosenmann† and P. Das

Electrical, Computer, and Systems Engineering Department
Rensselaer Polytechnic Institute
Troy, New York 12181

and

L. B. Milstein

Department of Electrical Engineering and Computer Sciences
University of California, San Diego
La Jolla, CA 92093

ABSTRACT

The effect of amplitude weighting of the received signal in a spread spectrum transform domain processing receiver is studied. Both experimental and theoretical results of probability error are given for direct sequence (DS) systems using a 63 chip spreading sequence with non-contiguous data. The DS signal is received in the presence of narrow-band interference and additive white Gaussian noise, and good agreement between theory and experiment is demonstrated. Results are given for both weighted and unweighted input signals at various notch bandwidths.

*This work was partially supported by the Army Research Office under Contract No. DAAG 29-81-K-0066.

†Presently with Armament Development Authority, Ministry of Defense, Haifa, Israel.

1. INTRODUCTION

The technique of transform domain processing for excision of narrow-band interference in a spread spectrum communication receiver has been analyzed in [1]-[2], and its processing gain advantages were described in [3]. Such a receiver has been implemented using SAW chirp devices, and the experimental results of the probability of error were presented in [4]. It was also shown that the experimental and theoretical results agree very well.

The results presented in [2]-[4] were for an unweighted observation period of T seconds. Therefore, the transform of the narrow-band interference has its spectrum as shown in Fig. 1. To reduce the sidelobes, the time-weighting function shown in Fig. 2 is used to observe the input waveform. It can be seen from Fig. 2 that the peak power limit of the weighting function is the same as that of the rectangular weighting. The transform of the weighted interference is shown in Fig. 3, where it can be seen the first side lobe has been noticeably reduced.

In Section 2, the implementation of the transform domain processing receiver for the excision of the narrow-band interference will be reviewed. In Section 3, both theoretical and experimental results of probability of the error are presented with both rectangular and cosine-squared time-weighting at the input. The desired signal is taken to be a 63 chip PN sequence, and results are given for different values of the excision filter notch width. Finally the conclusions are presented in Section 4.

2. THEORY OF THE RECEIVER WITH WEIGHTING

The transform domain processing receiver to be discussed is shown in Fig. 4. For the case of rectangular weighting the receiver has been

discussed in [1] and [2]. The received signal r(t) is composed of a direct sequence PSK waveform s(t).d(t), where s(t) is the spreading sequence and d(t) is the binary data, plus the additive white Gaussian noise n(t) and narrow-band interference I(t). The output of the receiver of Fig. 4 can be shown to be

$$g(T + T_1) = \int_0^T w(t)\ [s(t) + n(t) + I(t)]\ [h_R(t) * S(t)]\ dt$$

where $h_R(t)$ and s(t) are respectively the notch filter and the reference spreading sequence. From the above, the signal component of the final test statistic, the variance of the noise component and the interfered component can be shown to be given by

$$s_0 = \int_0^T w(t)\ s(t)\ [h_R(t) * s(t)]\ dt$$

$$\sigma_n^2 = \frac{\eta_0}{2} \int_0^T w^2(t)\ [h_R(t) * s(t)]^2\ dt$$

and

$$I_0 = \int_0^T w(t)\ \mathrm{Cos}[(\omega_0 + \delta\omega_0)t + \theta]\ [h_R(t) * s(t)]\ dt$$

respectively. For a seven chip PN sequence the terms in the bracket (i.e., $h_R(t) * s(t)$ is given in [1]. For other code lengths, the expression generalizes in an obvious manner.

3. THEORETICAL AND EXPERIMENTAL RESULTS

The results are given for a signal to interference ratio (SIR) of -20 dB, where the interference is a 14.992460 MHz single tone. To achieve

adequate phase averaging, the single tone interference is phase modulated with a phase excursion of $2\pi s$ radian at 100 Hz. The curves are parameterized by normalized offset frequency $\delta\omega_0$ from the carrier frequency and by the normalized single-sided notch-width $\delta\omega$.

Figs. 5-7 show curve of average probability of error versus energy-per-bit-to-noise spectral density ratio. These three figures are given for a constant two sided notch width of 3π (90 KHz) centered at 14.992460 MHz.

Fig. 5 shows both the theoretical and experimental results of probability of error when the input signal is time-weighted. It can be seen that the experimental results are in agreement with theory to within a fraction of a dB. In Figures 6 and 7 respectively, the theoretical and experimental results of P_e for weighted and unweighted input signal are presented. It can be seen again that the experimental and theoretical results agree very well.

In Fig. 8 the theoretical results of probability of error versus the notch bandwidth for the weighted and unweighted input signal at a constant signal-to-noise ratio of 10 dB is shown. From Figs. 8 and 9 the optimum two sided notch width for the weighted signal is 4π (60 KHz) whereas it is 12π (360 KHz) for the unweighted input signal. Also from Fig. 9 it can be seen that the experimental curve falls between the 10 dB and 9 dB theoretical curves.

The spread spectrum code used for this experiment is a 63 chip PN sequence with a chip rate of 1.875 MHz. The chirp devices which are used to perform the Fourier transforms in Fig. 4 have a center frequency of 15 MHz, bandwidth of 7 MHz, interaction time of 117 μsec and chirp rate of 3.0E 10 Hz/sec. Finally the observation period T is 33.6 μsec. The

transform variable (ω) is related to time through $\omega = 2\beta t$ where β is the chirp rate. Thus in the ω domain 1 μsec corresponds to 60 KHz.

4. CONCLUSION

Both theoretical and experimental results of probability of error were presented for a transform domain processing receiver using time-weighting of the input signal. It was seen that the theoretical results were in good agreement with the experimental results for both the weighted and unweighted input signal. The most important conclusion is that the use of weighting does not appear to buy anything in terms of improved system performance.

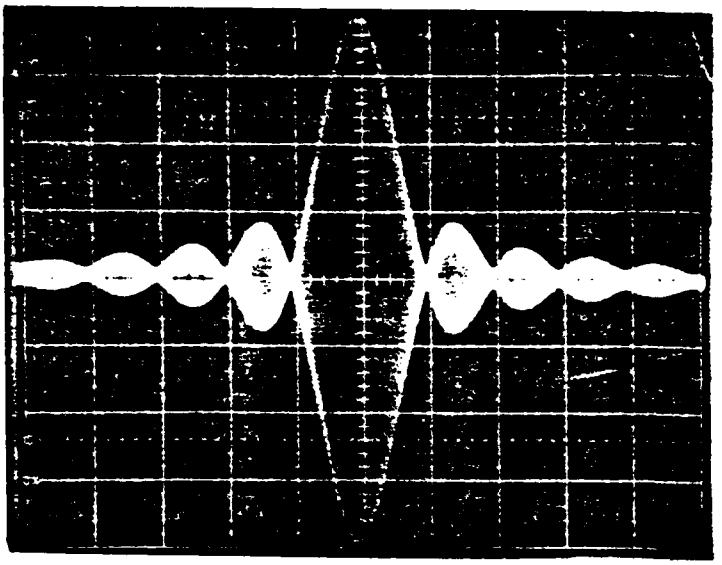

Figure 1

Transform of Interference at
14.992460 MHz
30 KHz/box

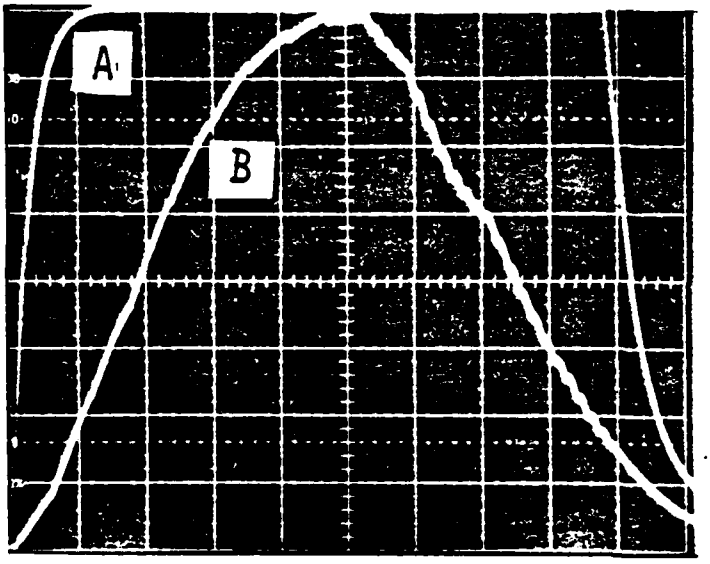

Figure 2

Trace A) Rectangular Weighting
B) Weighting Function

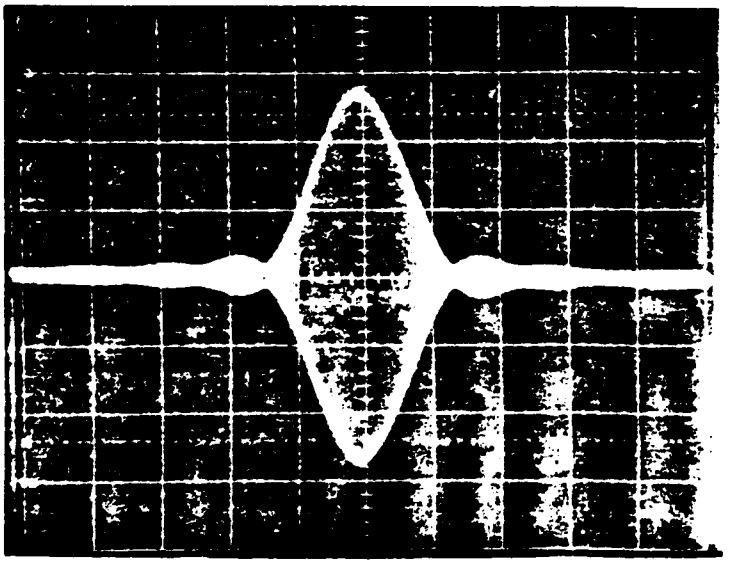

Figure 3

Transform of Weighted Interference
(same scale as Fig. 1)

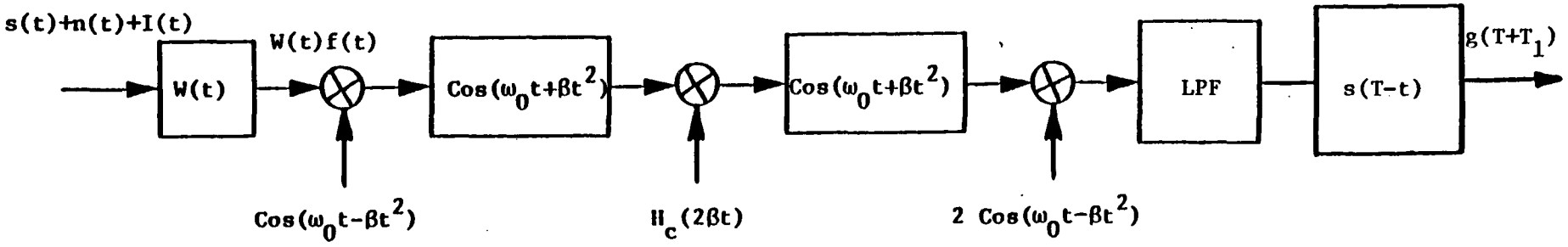

Figure 4 Transform Domain Filtering Receiver

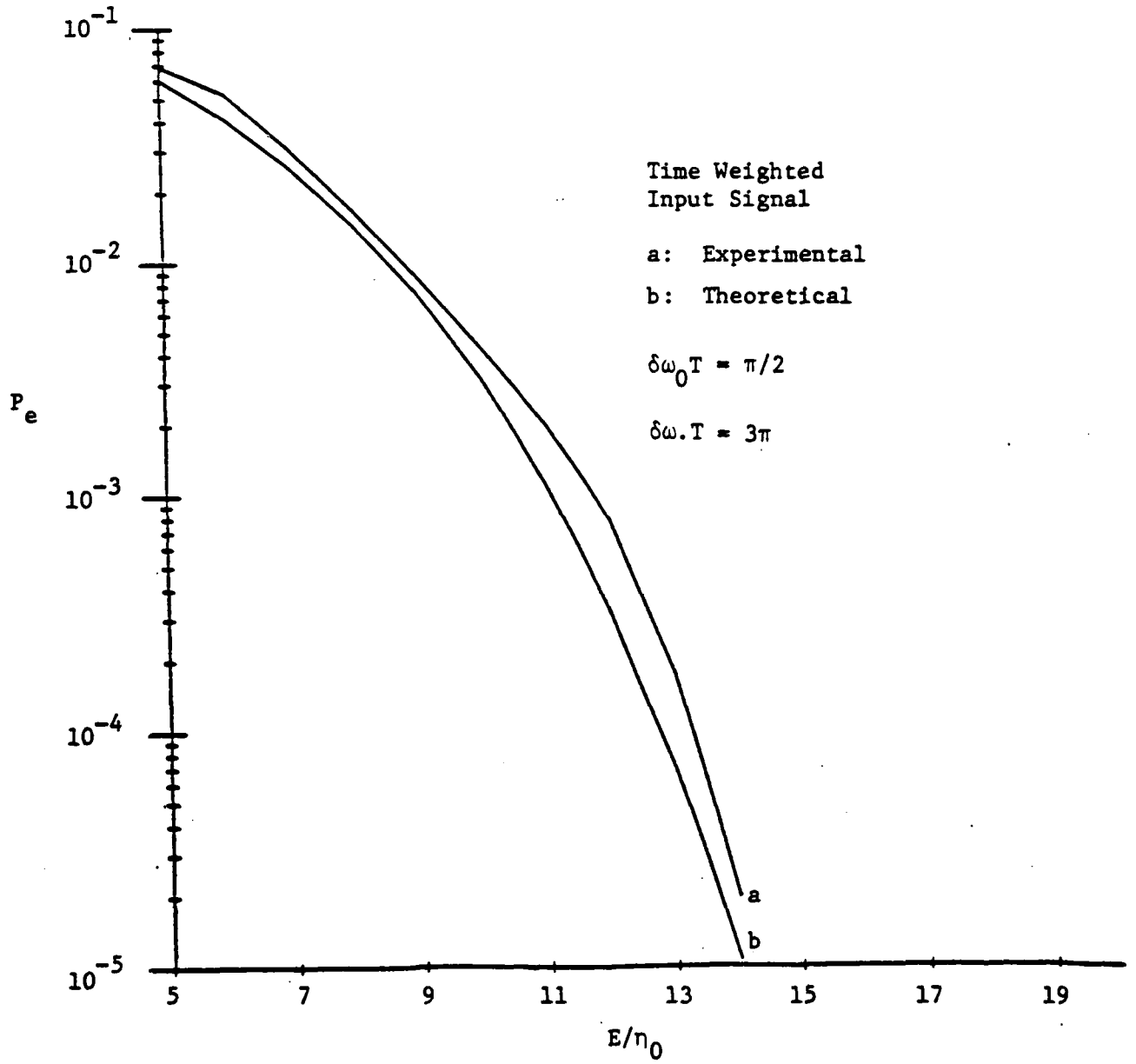

Figure 5 Probability of Error Versus E/η_0

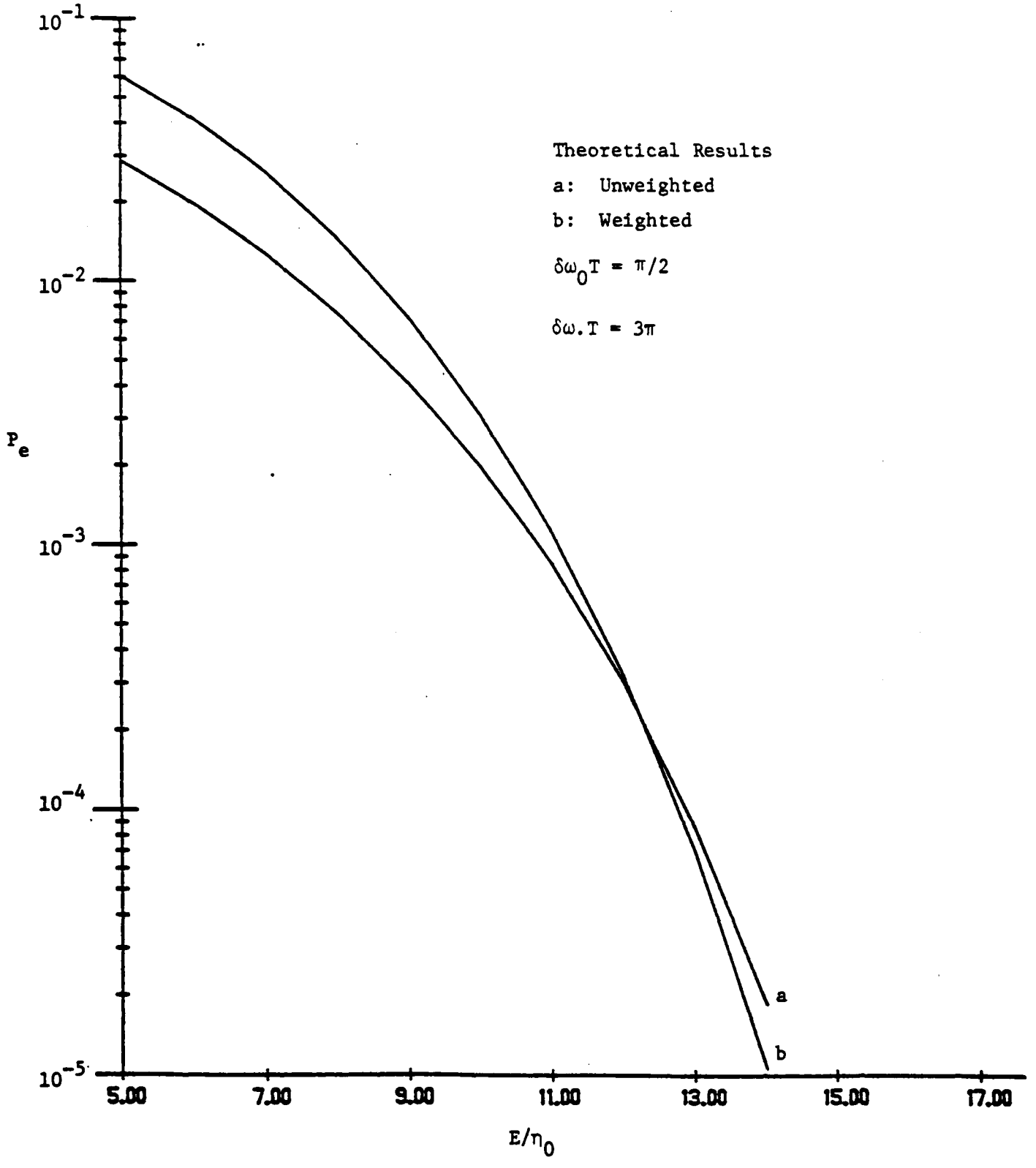

Figure 6 Probability of Error Versus E/η.

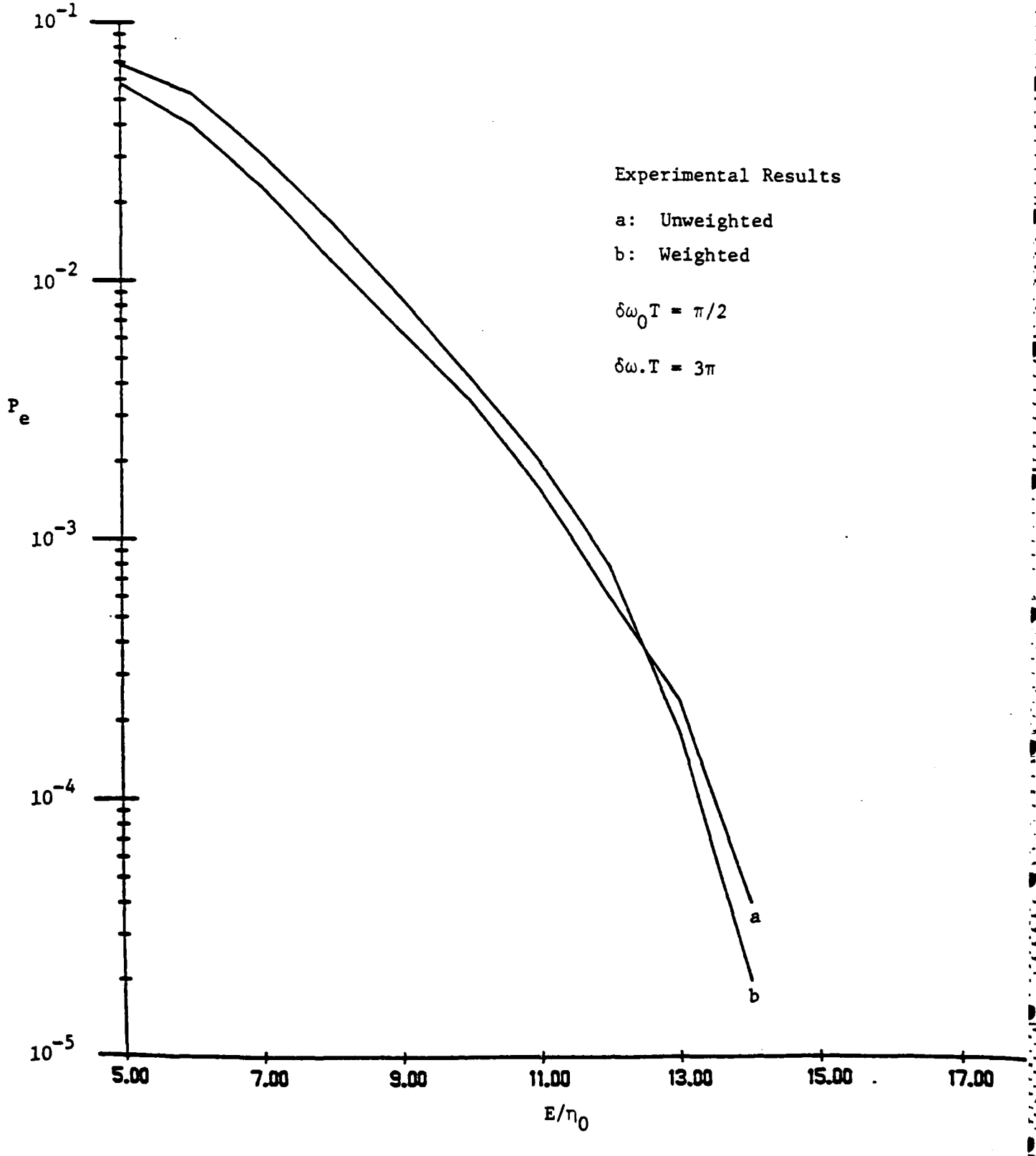

Figure 7 Probability of Error Versus E/η_0.

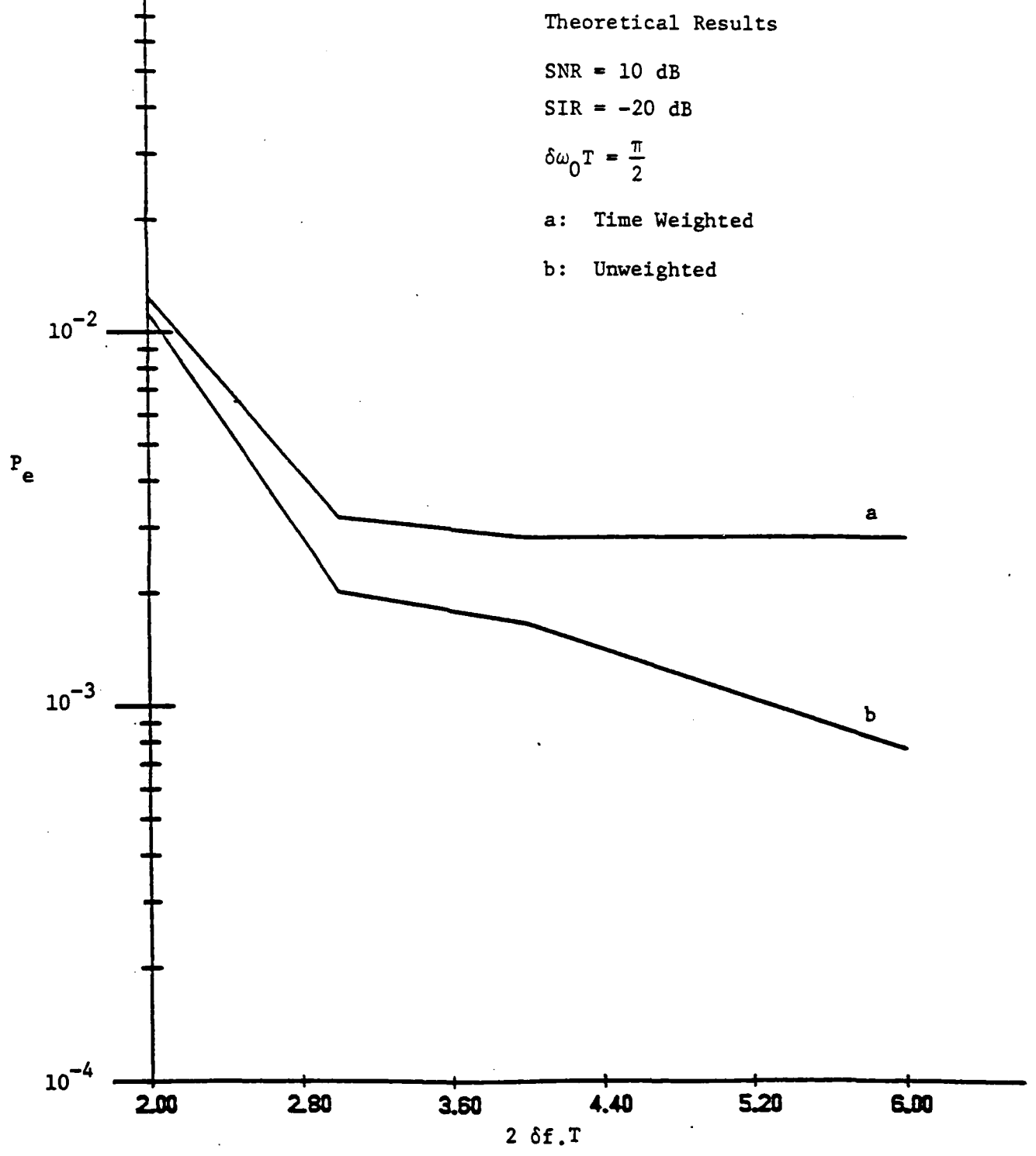

Figure 8 Probability of Error Versus the Two Sided Notch Width Times Symbol Duration.

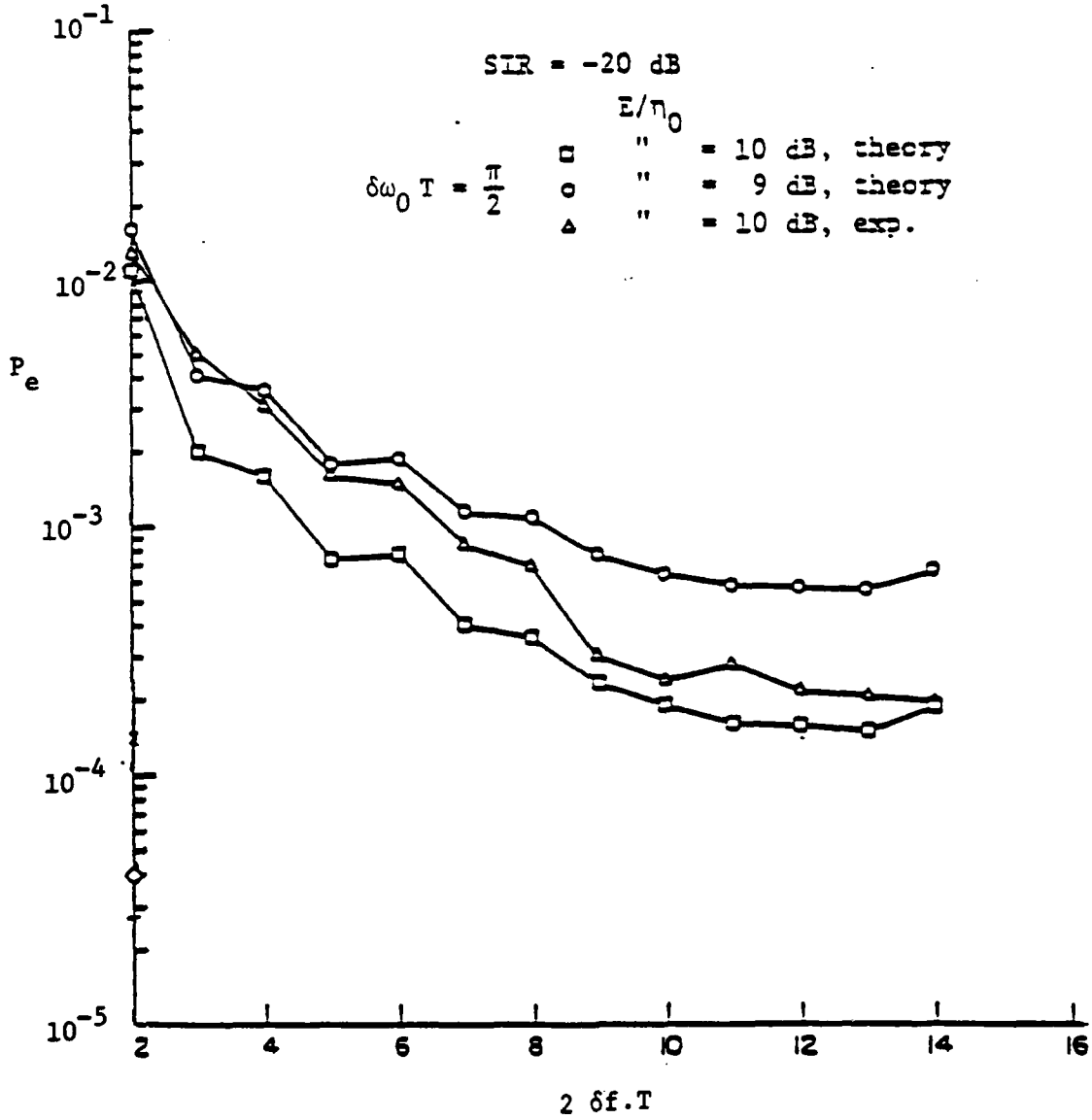

Figure 9 Probability of Error Versus the Two Sided Notch Width Times Symbol Duration.

REFERENCES

[1] L. B. Milstein and P. Das, "An Analysis of a Real Time Transfor Domain Filtering Digital Communication System - Part I", IEEE Trans. Commun., Vol. COM-28, No. 6, pp. 816-824, June 1980.

[2] P. Das, L. B. Milstein and D. R. Arsenault, "Adaptive Spread Spectrum Receiver Using SAW Technology", IEEE Trans. Comm., Vol. COM-25, pp. 841-847, August 1977.

[3] L. B. Milstein, P. Das and J. Gevargiz, "Processing Gain Advantages of Transform Domain Filtering DS-Spread Spectrum Systems", MILCOM 82, pp. 21.2.1-21.2.5, 1982.

[4] M. Rosenmann, J. Gevargiz, P. K. Das and L. B. Milstein, "Probability of Error Measurement for an Interference Resistant Transform Domain Processing Receiver", MILCOM 83, pp. 636-640, 1983.

APPENDIX D

RAPID ACQUISITION FOR DIRECT SEQUENCE SPREAD SPECTRUM COMMUNICATIONS USING PARALLEL SAW CONVOLVERS

by

Laurence B. Milstein
Dept. Electrical Engineering & Computer Sciences
University of California, San Diego
La Jolla, CA 92093

John Gevargiz and Pankaj K. Das
Electrical, Computer & Systems Engineering Dept.
Rensselaer Polytechnic Institute
Troy, NY 12181

ABSTRACT

In this paper, a technique will be described which uses multiple surface acoustic wave (SAW) devices in parallel to reduce the acquisition time of a direct sequence spread spectrum communication system. Analysis of system performance in both the search and lock modes will be presented, and key quantities such as probability of false alarm, probability of correct detection, mean dwell time and mean time to lose lock will be derived.

*This work was partially supported the the U.S. Army Research Office under Grant DAAG 29-81-K-0066.

1. INTRODUCTION

In this paper, a rapid acquisition technique based upon the use of parallel processing the received waveform of a direct sequence spread spectrum communication system with multiple surface acoustic wave (SAW) convolvers will be presented. Because the processing is indeed done in parallel, a decrease in acquisition time from a comparable serial search scheme is achieved.

A derivation of the probabilities of false alarm and correct detection for both the search mode and the lock mode are presented, as well as a Markov chain analysis of an overall search-lock strategy. Expressions are derived for such key system parameters as probability of losing lock and average time to loss of lock. Finally, some numerical results are presented showing the variation of false alarm and detection probabilities with the number of parallel convolvers and with the ratio of received energy-per-bit-to-noise spectral density.

The paper is divided into six sections, with a description of the system presented in the next section, the derivations of probability of false alarm and probability of correct detection presented in Section 3, a Markov chain analysis of the search and lock modes behavior given in Section 4, and numerical results given in Section 5. Conclusions are then presented in the last section.

2. SYSTEM DESCRIPTION

The acquisition scheme can be best described by referring to Fig. 1. There are two modes of operation, a search mode and a lock mode. Consider the search mode first, during which all switches are in position 1. (Ignore, for the moment, the recirculating delay line circuit at the input to the system.) Notice that there are N convolvers, each of duration 2T seconds, where it is assumed that M chips of the spreading sequence span T seconds. The

full period of the spreading sequence, L, is divided into subsequences each of length M, and for simplicity, it is assumed that $\frac{L}{M}$ is an integer.

Each of the N convolvers has as a reference input one of the subsequences of length M. Initially, let us assume that the total phase uncertainty at the start of acquisition, say K chips, is spanned by the MN phase positions of the N convolvers. (Notice that even if L is much greater than MN, this uncertainty condition could still be satisfied.) This guarantees that the correct phase position of the received waveform is "seen" by one of the N convolvers somewhere in the integration interval of the convolvers.

The convolver outputs are sampled at times $t = T + jT_c$, where $T = MT_c$ and $j = 0, 1, \ldots, M - 1$. The length of each convolver is chosen to be 2T. With these parameter values, if the N reference inputs enter the convolvers at $t = 0$, the unknown phase position will overlap the correct phase reference of one of the N convolvers at some time during the interval $t \in [MT_c, (2M - 1)T_c] = [T, 2T - T_c]$. After sampling, the largest of the resulting MN samples is chosen as the correct phase of the incoming waveform. Since one of the MN samples is the correct sample, it is therefore possible to initially acquire in 2T seconds. The actual mechanism for making the final decision regarding acquisition will be described in the next section.

Suppose now that the initial phase uncertainty K is greater than MN. For this case, the recirculating delay line, shown in Fig. 1, is used at the input to the system with both switches A and B closed. On the input side, after the first T second segment of the received waveform is in the system, switch A is opened and the T-second segment is recirculated J times, where

J equals $[\frac{K}{MN}]$, and [x] is the smallest integer greater than or equal to x. On the reference side, the first N subcodes are put through the respective convolvers during the interval [0, T]. From [T, 2T], no reference input is used, but from [2T, 3T], the next N subcodes are used as reference inputs. In general, the i^{th} set of N subcodes, i=1, ..., J, is used as reference inputs during the interval [(i-2)T, (i-1)T].

Considering next the lock mode, switch A is kept closed, switch B is kept open, and all other switches that were in position 1 are now put in position 2, so that each convolver output passes through the appropriate delay line. (Note that the recirculating delay line at the convolver input is not used.) In this mode of operation, the N outputs are noncoherently summed to yield an effective increase in integration time over that used in the search mode. To reset the reference input during the lock mode simply requires separating successive subcodes into any of the N convolvers by NT seconds.

Notice that when the system is locked to the correct phase position, all the inputs to the delay lines have been despread and hence the delay lines themselves do not have to be broadband devices. Similarly, if an incorrect phase position is being observed, while the inputs to the delay lines will no longer be despread, using narrowband delay lines will still not result in any performance degradation since under this latter condition, a signal component out of the delay lines is not wanted.

3. PERFORMANCE ANALYSIS

Let the reference input to the i^{th} convolver be denoted by $PN_{(i-1)M+1}(t)$, where $PN_k(t)$ denotes a segment of a longer pseudonoise sequence (denoted PN(t)) from $(k-1)T_c$ to $(k-1+M)T_c$, M is the number of chips

in each subcode and T_c is the duration of each chip. Therefore, $PN_{(i-1)M+1}(t)$ is a subcode in the interval $[(i-1)MT_c, iMT_c]$, $i = 1,2, \ldots, N$. For simplicity in notation in what follows, the reference subcode $PN_{(i-1)M+1}(t)$ will be denoted by $PN_i^{(R)}(t)$. (Note that we have arbitrarily defined the start of subcode $PN_1^{(R)}(t)$ to correspond to t=0.)

To determine the probability that the correct phase position has been found, assume that $PN_j(t)$ is the subcode that is currently being received, and to be specific, assume the received subcode $PN_j(t)$ plus noise enters the left side of the convolvers of Figure 1 at the same instant of time that the reference subcodes $PN_i^{(R)}(T-t)$, $i = 1, \ldots, N$ enter the right side. (Note that by making the convolver length equal to 2T, it is not necessary to have synchronism between the start of a received subcode and the start of the reference codes; it is done here only for convenience.) Also, for simplicity, assume $J = 1$. If we concentrate on the i^{th} convolver, then from [1], it is straightforward to show that at any time $t\varepsilon[T, 2T]$, the convolver output is given by

$$U_i(t) = \int [APN_j(\tau)\cos w_o\tau + n(\tau)]\ PN_i^{(R)}(-2t + T_1 + T + \tau) \cdot \cos[w_o(\tau - 2t) + \phi]\ d\tau \qquad (1)$$

where T_1 is the length of the convolver, A is a constant amplitude, ϕ is a random phase uniformly distributed in $[0, 2\pi]$ and n(t) is AWGN of two-sided spectral density $\frac{\eta_0}{2}$. The specific limits of integration of (1) depend upon the degree of overlap between the received waveform and the reference code. If we assume the received waveform has completely occupied the convolver when the subcodes first enter, then for $t\varepsilon[T, 2T]$, the limits are 0 to T.

If double frequency terms are ignored in the integrals and if T_1 is set equal to 2T, then (1) reduces to

$$U_i(t) = \frac{1}{2}\int_0^T A \cdot PN_i^{(R)}(-2t + 3T + \tau)\, PN_j(\tau)\, d\tau \cos(2w_0 t - \phi)$$

$$+ \int_0^T PN_i^{(R)}(-2t + 3T + \tau) \cos(w_0\tau) n(\tau)\, d\tau \cos(2w_0 t - \phi)$$

$$+ \int_0^T PN_i^{(R)}(-2t + 3T + \tau) \sin(w_0\tau) n(\tau)\, d\tau \sin(2w_0 t - \phi) \tag{2}$$

Assuming initially that i = j and that the sampling time T_s corresponds to precisely sampling the correct convolver at the peak of its response, then

$$U_j(T_s) = [\tfrac{1}{2} AT + N_{c_j}(T_s)] \cos[2w_0(T_s) - \phi]$$

$$+ N_{s_j}(T_s) \sin[2w_0(T_s) - \phi] \tag{3}$$

where

$$N_{c_j}(T_s) \triangleq \int_0^T PN_j^{(R)}(\tau) n(\tau) \cos w_0\tau d\tau \tag{4}$$

and

$$N_{s_j}(T_s) \triangleq \int_0^T PN_j^{(R)}(\tau) n(\tau) \sin w_0\tau d\tau\ . \tag{5}$$

Both $N_{c_i}(T_s)$ and $N_{s_i}(T_s)$ are zero-mean Gaussian random variables with variance $\frac{\eta_0 T}{4}$. They are also statistically independent.

For $i \neq j$ the output of the convolver at the sampling instant is given by

$$U_i(T_s) = [\tfrac{1}{2} AR_{ij} + N_{c_i}(T_s)] \cos[2w_0(T_s) - \phi]$$

$$+ N_{s_i}(T_s) \sin[2w_0(T_s) - \phi] \qquad (6)$$

where $N_{c_i}(T_s)$ and $N_{s_i}(T_s)$ have the same statistical properties as $N_{c_j}(T_s)$ and $N_{s_j}(T_s)$, and where

$$R_{ij} \triangleq \int_0^T PN_i^{(R)}(t)\, PN_j(t)\, dt \qquad (7)$$

Finally, with an appropriate change of notation, (6) can be seen to apply to the output of any of the N convolvers at any of the M-1 incorrect sampling times. Therefore, if the output of the i^{th} square-law detector at the k^{th} sampling time is denoted by $S_i(T + kT_c)$, and if the correct sampling time (which equals $\frac{3T}{2}$ for the specific timing being used here) corresponds to $k = k_c$, then an error will occur if

$$S_i(T + kT_c) > S_j(T + k_cT_c) \text{ for any } k,\ i \neq j,$$

or if

$$S_j(T + kT_c) > S_j(T + k_cT_c) \text{ for } k \neq k_c.$$

These conditions correspond to an incorrectly matched convolver at any sampling time having an output larger than that of the correct convolver at the correct sampling time, and to the correct convolver having a larger output at some time other than the correct sampling time, respectively.

Denoting by $\{S_m\}$, $m = 1, \ldots MN - 1$, the set of samples of either $S_i(T + kT_c)$ for any k or $S_j(T + kT_c)$ for $k \neq k_c$, and denoting $S_j(T + k_cT_c)$ by S_0, then an error occurs if $S_m > S_0$ for any m. Hence the probability of error in the search mode, $P_e^{(s)}$, can be upper bounded by

$$P_e^{(s)} = P\{(S_i > S_0) \text{ or } (S_2 > S_0) \text{ or } \ldots. \text{ or } (S_{MN-1} > S_0)\}$$

$$\leq \sum_{i=1}^{MN-1} P\{S_i > S_0\} \tag{8}$$

If $P_{ij} \triangleq P\{S_i > S_j\}$, then P_{ij} can be shown to be given by ([2])

$$P_{ij} = \frac{1}{2}\left[1 - Q(\sqrt{b}, \sqrt{a}) + Q(\sqrt{a}, \sqrt{b})\right] \tag{9}$$

where

$$\begin{Bmatrix} a \\ b \end{Bmatrix} \triangleq \frac{1}{2}\left[\frac{2\sigma^2(A^2R_{ij}{}^2 + A^2T^2) - 4\sigma^2\rho_{ij}A^2R_{ij}T}{(2\sigma^2)^2 - 4(\rho_{ij}\sigma^2)^2}\right.$$

$$\left. \pm \frac{A^2R_{ij}{}^2 - A^2T^2}{[4\sigma^4(1 - \rho_{ij}{}^2)]^{1/2}}\right] = \left(\frac{AT}{2\sigma}\right)^2\left[1 \mp (1 - \rho_{ij}{}^2)^{1/2}\right] \tag{10}$$

$$Q(a,b) \triangleq \int_b^\infty x\, e^{-\frac{a^2+x^2}{2}} I_0(ax)\, dx \tag{11}$$

$$\sigma^2 \triangleq \eta_0 T \tag{12}$$

$$\rho_{ij}\sigma^2 \triangleq \eta_0 R_{ij} \tag{13}$$

and $I_0(x)$ is the modified Bessel function of the first kind and zeroth order.

As a special case, if all the ρ_{ij} are approximately zero, then P_{ij} reduces to

$$P_{ij} = \frac{1}{2} e^{-\frac{E}{2\eta_0}} \tag{14}$$

and (8) reduces to

$$P_e^{(s)} \leq (NM - 1)\,\frac{1}{2}\,e^{-\frac{E}{2\eta_0}} \tag{15}$$

In (14) and (15), $E = \frac{A^2T}{2}$ and is the energy-per-integration interval, T, of the transmitted signal. As a final observation for the search mode analysis, note that for this special case (all $\rho_{ij} = 0$), the exact probability of error can be found ([3]) and is given by

$$P_e^{(s)} = 1 - \sum_{i=0}^{NM-1} \binom{MN-1}{i} \frac{(-1)^{NM-1-i}}{NM - 1} \exp\left[-\frac{E}{\eta_0}\frac{MN - i - 1}{NM - i}\right] \tag{16}$$

Consider now the lock mode, in which all the switches in Figure 1 are set at position 2. In this latter mode, the N convolver outputs are all appropriately delayed and summed, but only at a specific phase position decided upon in the search mode.

To analyze the performance of the system in the lock mode, the approximation that all the $\rho_{ij} = 0$ was made in order to simplify the analysis. With this approximation, it can be seen that when an incorrect phase position is being observed, the decision variable has a central chi-square distribution with 2N degrees-of-freedom, and when the correct phase position is being observed, the decision variable has a non-central chi-square distribution with 2N degrees-of-freedom and noncentrality parameter $a_1^2 = NA^2T^2$. Therefore, the probabilities of false alarm and correct detection in the lock mode are given by

$$P_{fa}^{(\ell)} = \int_{\lambda}^{\infty} \frac{1}{(2\eta_0 T)^N \Gamma(N)}\, y^{N-1}\, e^{-\frac{y}{2\eta_0 T}}\, dy \tag{17}$$

and

$$P_d^{(\ell)} = \int_{\lambda}^{\infty} \frac{1}{2\eta_0 T} \left(\frac{y}{a_1^2} \right)^{\frac{N-1}{2}} e^{-\frac{y+a_1^2}{2\eta_0 T}} I_{N-1}\left(\frac{a_1\sqrt{y}}{\eta_0 T} \right) dy \qquad (18)$$

respectively, where γ is the threshold, $\Gamma(.)$ is the gamma-function and $I_{N-1}(.)$ is a modified Bessel function.

4. SEARCH MODE AND LOCK MODE TRANSITIONS

In order to complete both the system description and the performance analysis, the specific procedure for transitioning from one phase position to the next in the search mode must be specified, as well as the procedure for transitioning from the search mode to the lock mode. Towards this end, a search-lock strategy similar to that described in [4] will be used. In particular, once a phase position has been decided upon in the search mode, two more successive "hits" at that phase position will be required in order to enter into the lock mode. That is, once all phase positions within the uncertainty range have been examined and an initial decision made as to which is the correct position, the procedure is repeated two more times. If the same relative phase position is chosen both times, the system advances to the lock mode. Similarly, two successive "misses" in the lock mode will be necessary in order for that phase position to be rejected and the search mode reinitiated. However, in the lock mode, only the specific phase position previously decided upon in the search mode is examined, not all possible phase positions falling within the uncertainty region.

A flow diagram of this procedure is shown in Fig. 2. It is well known (see, e.g., [4], [5]) that this type of process can be modeled as a

finite Markov chain with absorbing boundaries. From Fig. 2, it is seen that there are six states to this particular Markov chain, labelled 1 to 6. States 1 and 6 are designated R for "rejection", meaning when either state is reached, the phase position currently being examined is rejected (i.e., the Markov chain has reached one of its absorbing states). States S1 and S2 correspond to the two search mode states, whereas L1 and L2 correspond to the two lock mode states.

In Fig. 2, P_s denotes either $P_e^{(s)}$ or $1 - P_e^{(s)}$ (depending upon whether the phase under consideration is incorrect or correct, respectively) and P_L represents $P_{fa}^{(\ell)}$ or $P_d^{(\ell)}$ under similar circumstances for the lock mode. Using the absorbing Markov chain model for this system, the canonical form for the transition matrix, described in [4] and [5], is shown below.

$$\bar{\bar{P}} = \begin{array}{c} \\ 1 \\ 6 \\ 2 \\ 3 \\ 4 \\ 5 \end{array} \left[\begin{array}{cc|cccc} 1 & 6 & 2 & 3 & 4 & 5 \\ \hline 1 & 0 & 0 & 0 & 0 & 0 \\ 0 & 1 & 0 & 0 & 0 & 0 \\ \hline 1-P_s & 0 & 0 & P_s & 0 & 0 \\ 0 & 0 & 1-P_s & 0 & P_s & 0 \\ 0 & 0 & 0 & 0 & P_L & 1-P_L \\ 0 & 1-P_L & 0 & 0 & P_L & 0 \end{array}\right] = \left[\begin{array}{c|c} \bar{\bar{S}} & \bar{\bar{\phi}} \\ \hline \bar{\bar{R}} & \bar{\bar{Q}} \end{array}\right] \tag{19}$$

Forming the matrix

$$\bar{\bar{I}} - \bar{\bar{Q}} = \begin{bmatrix} 1 & -P_s & 0 & 0 \\ (1-P_s) & 1 & -P_s & 0 \\ 0 & 0 & 1-P_L & -(1-P_L) \\ 0 & 0 & -P_L & 1 \end{bmatrix} \tag{20}$$

where $\bar{\bar{I}}$ is an identity matrix, and defining the new matrix

$$\bar{\bar{B}} = [I - Q]^{-1} \bar{\bar{R}},$$

it is shown in [4] that the probability of losing lock is given by entry b_{26} of the above $\bar{\bar{B}}$ matrix. Notice that the notation b_{26} refers to elements of the $\bar{\bar{R}}$ matrix. That is, the rows of $\bar{\bar{B}}$ are numbered 2, 3, 4 and 5, and the columns of $\bar{\bar{B}}$ are numbered 1 and 6. For the system being considered here, the probability of losing lock is given by

$$b_{26} = \frac{P_s^2}{1 - P_s(1 - P_s)} \tag{21}$$

In addition to the probability of losing lock, other quantities of interest are the mean dwell time in an incorrect phase position and the expected time to loss of lock, given that the system is in state L2 at the correct phase position. From [4] and [5], it is shown that if τ_j is the mean time to arrive at any absorbing state given an initial transient state j (e.g., S1), then the vector of elements τ_j, denoted $\bar{\tau}$, is given by

$$\bar{\tau} = \begin{bmatrix} \tau_2 \\ \tau_3 \\ \tau_4 \\ \tau_4 \end{bmatrix} = [\bar{\bar{I}} - \bar{\bar{Q}}]^{-1} \bar{\lambda} , \tag{22}$$

where $\bar{\lambda}$ is a vector whose elements are the times needed to make each transition.

Since the time needed to move from one state to the next state is 2TK in the search mode and (N+1)T in the lock mode, it can be shown in a straightforward manner that the mean dwell time is given by

$$\tau_2 = \frac{2K(1 - P_L)^2 (1 + P_s) + (N+1) P_s^2 (2 - P_L)}{(1 - P_L)^2 [1 - P_s(1 - P_s)]} T \tag{23}$$

and the expected time to loss of lock is given by

$$\tau_4 = \frac{2 - P_L}{(1 - P_L)^2} (N+1)T \tag{24}$$

5. NUMERICAL RESULTS AND DISCUSSION

As a specific example, it will be assumed that a PN sequence of length L=1023 is being received simultaneously in N=11 convolvers, thereby resulting in M=93 unknown phase positions in each convolver. If the approximation leading to (14)-(16) is used, namely that all the ρ_{ij} of (13) are zero, the curve of $P_e^{(s)}$ shown in Fig. 3 results. For the same system in the lock mode, Fig. 4 shows results of $P_d^{(\ell)}$ for various values of γ (or equivalently for various values of $P_{fa}^{(\ell)}$).

The variations of P_{fa} and P_d with N are illustrated in Figures 5-9. Fig. 5 shows $P_{fa}^{(s)}$ versus E/η_0 for three values of N, N=5, 10 and 15. Similar results for $P_d^{(\ell)}$ are presented in Fig. 6, and Figs. 7-9 show how $P_d^{(\ell)}$ varies with $P_{fa}^{(\ell)}$ for a given value of N.

As a perspective on the effect of approximating the ρ_{ij} by zero for $i \neq j$, the exact P_{ij} of (9) were computed, and some of the results are shown in Fig. 10. For the same PN sequence of length L=1023 referred to above, a specific subsequence of length M=93 was fed into all eleven convolvers and the resulting 1023 values of ρ_{ij} were computed. That is, the starting phase of the reference input sequence $PN_i^{(R)}(t)$ took values 0, 93 T_c, ... 930 T_c, corresponding to (i = 1, 2, ... 11), where i is the index of the convolver. Also, the phases of $PN_j(t)$, the input sequence, took values 0, T_c, 2 T_c ... 92 T_c, corresponding to j = 1, 2, 3, ... 93. Hence ρ_{ij} was calculated for all these combinations of i and j over the observation period T, and these ρ_{ij} were then used to compute the corresponding values of P_{ij}.

There are four curves of P_{ij} along with their corresponding values for ρ_{ij} shown in Fig. 10. These curves correspond to (i,j) pairs of (2,1), (3,1), (4,1) and (1,3). With the notation introduced above, (2,1) corresponds to the P_{ij} of the second convolver when the starting phase of its input signal is zero and that of its reference is 93 T_c. Similarly, (1,3) corresponds to the first convolver when its input has a starting phase of 2 T_c and its reference a starting phase of zero. The maximum variations in P_{ij} shown by these curves at any given SNR come very close to the largest variation in P_{ij} when all possible (i,j) combinations are considered.

Also plotted on this figure is the curve corresponding to $\rho_{ij} = 0$ (i.e., $\frac{1}{2} e^{-\frac{1}{2} SNR}$). Upon comparing these curves, it can be seen that, at least for this one example, the probability of error generated by approximating the ρ_{ij} by zero falls somewhere between the upper and lower values of P_{ij} for SNR between about 8 and 13 dB, corresponding to a P_{ij} between about 2×10^{-2} and 2×10^{-5}. In particular, the approximate value is within a factor of two of either the largest or smallest value for SNR = 9 dB, and within a factor of five (approximately) at SNR = 13 dB.

If the curves of probability of error are examined, it will be seen that the price one is paying for the decrease in acquisition time is either an increase in probability of false alarm in the search mode at a given E/η_0 (relative to a classical serial search strategy), or an increase in required E/η_0 to yield a prespecified probability of false alarm. This is to be expected, since in the search mode, a decision is made by comparing JMN voltage samples with one-another. That is, there are JMN-1 incorrect phase positions present and the probability that the samples corresponding to at least one of them will exceed the value of the sample corresponding

to the correct phase position increases as JMN increases, for a given E/η_0.

The advantage of the scheme, of course, is that in 2T seconds, MN phase positions are examined. In a standard serial search technique, examining MN phase positions requires MNT seconds, and so an improvement of a factor of MN/2 is achieved. However, it is still necessary to have an acceptable probability of error in the search mode, and if the E/η_0 required to yield a given level of performance is too large, one can always increase the number of states in the search mode. While this will not decrease $P_e^{(s)}$ on any given try, it <u>will</u> decrease the probability of entering lock at an incorrect phase position. Also, this further illustrates a point made in [4], namely that a large integration time in the lock mode is desirable (recall that in the scheme described here, the integration time in the lock mode of any one convolver is the same as it is in the search mode, namely T seconds, but that noncoherently summing N output samples has the effect of yielding a larger integration time). Since one has to search <u>all</u> the phase positions in the uncertainty region in the search mode, but one only has to check a single phase position in the lock mode, once one has entered the lock mode, it is desirable to stay in that mode (i.e., not lose lock) for as long as possible. As long as the overall mechanism of entering the lock mode results in a correct decision with a reasonably high probability, the additional time spent in false lock caused by employing this strategy can be kept to a tolerable level.

Finally, it is at times more meaningful to consider such parameters as mean-dwell time at an incorrect phase position and mean-time to loss-of-lock at the correct phase position than it is to consider the probabilities

of detection and false-alarm. (Which set of parameters is more relevant to a given system is typically a function of how long the acquisition sequence is available, with the former parameters being more significant in continuously running sequences as in certain navigation systems and the latter parameters being more significant in more bursty systems such as packet radios.) To illustrate the behavior of this particular acquisition scheme with respect to mean-dwell time and mean-time to loss-of-lock, consider Figs. 11 and 12. In Fig. 11, $\frac{\tau_2}{T}$ is plotted versus the false alarm probability in the search mode, with the false alarm probability in the lock mode as a parameter. In Fig. 12, $\frac{\tau_4}{T}$ is plotted versus the probability of correct detection in the lock mode.

6. CONCLUSION

A technique for the rapid acquisition of a DS spread spectrum signal has been presented. The scheme relies on parallel processing different subcodes of a longer spreading sequence simultaneously in SAW convolvers, and results in a reduction of search time which is proportional to M times N, where M is the number of chips being processed in each convolver and N is the number of convolvers. Results were presented for such key system parameters as probability of detection and mean-time to loss-of-lock. While only analytical results were considered in the paper, it is believed that the system could be implemented with current technology in SAW devices.

REFERENCES

[1] L. B. Milstein and P. K. Das, "Spread Spectrum Receiver Using Surface Acoustic Wave Technology," IEEE Trans. Comm., Vol. COM-25, August 1977, pp. 841-847.

[2] M. Schwartz, W. R. Bennett and S. Stein, Communication Systems and Techniques. McGraw-Hill, 1966, Ch. 8.

[3] A. J. Viterbi, Principles of Coherent Communication, McGraw-Hill, 1966, Ch. 8.

[4] P. M. Hopkins, "A Unified Analysis of Pseudonoise Synchronization by Envelope Correlation," IEEE Trans. Comm., Vol. COM-25, August 1977, pp. 770-778.

[5]. J. G. Kemeny and J. L. Snell, Finite Markov Chains, Van Nostrand, 1969.

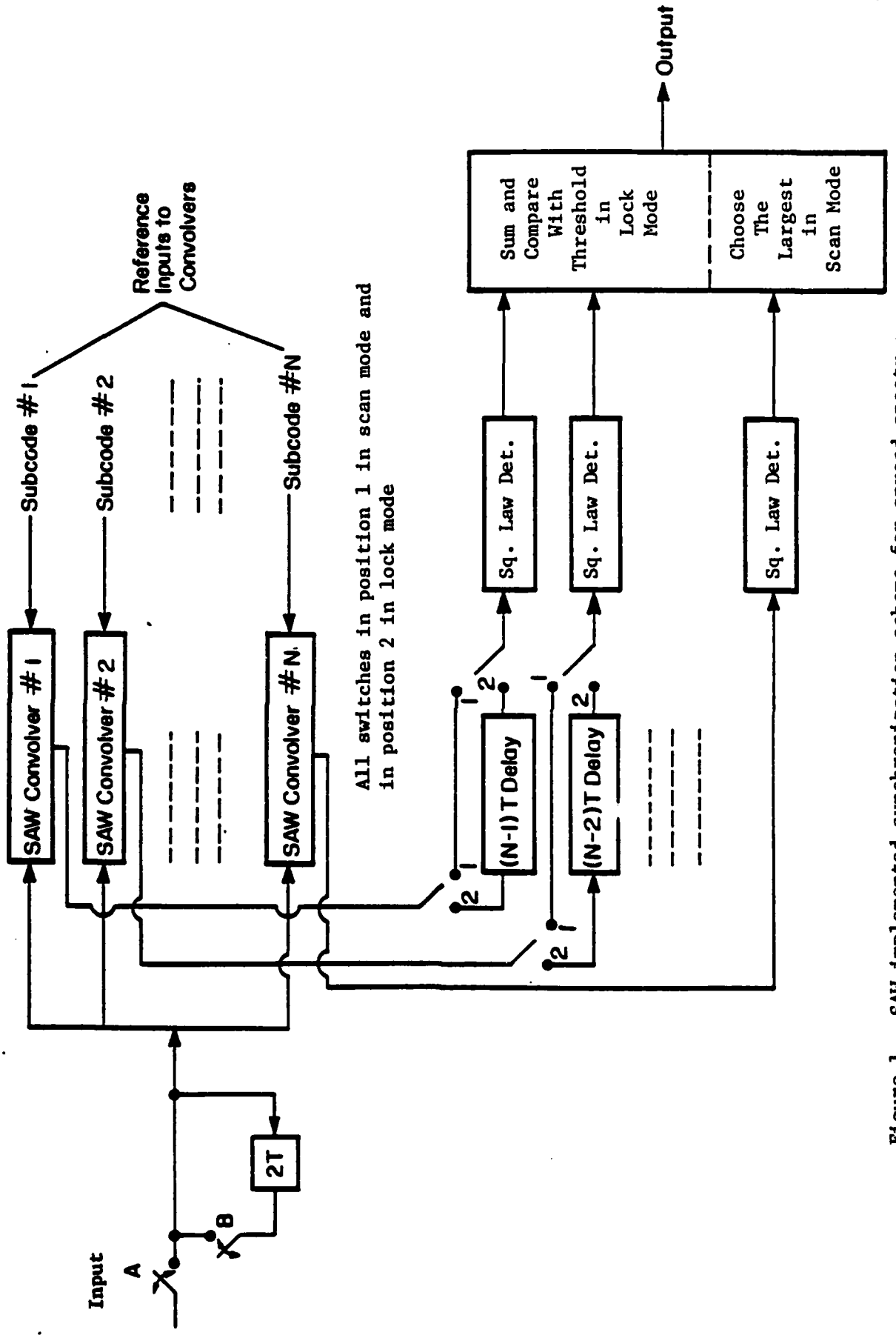

Figure 1. SAW-implemented synchronization scheme for spread spectrum Receiver.

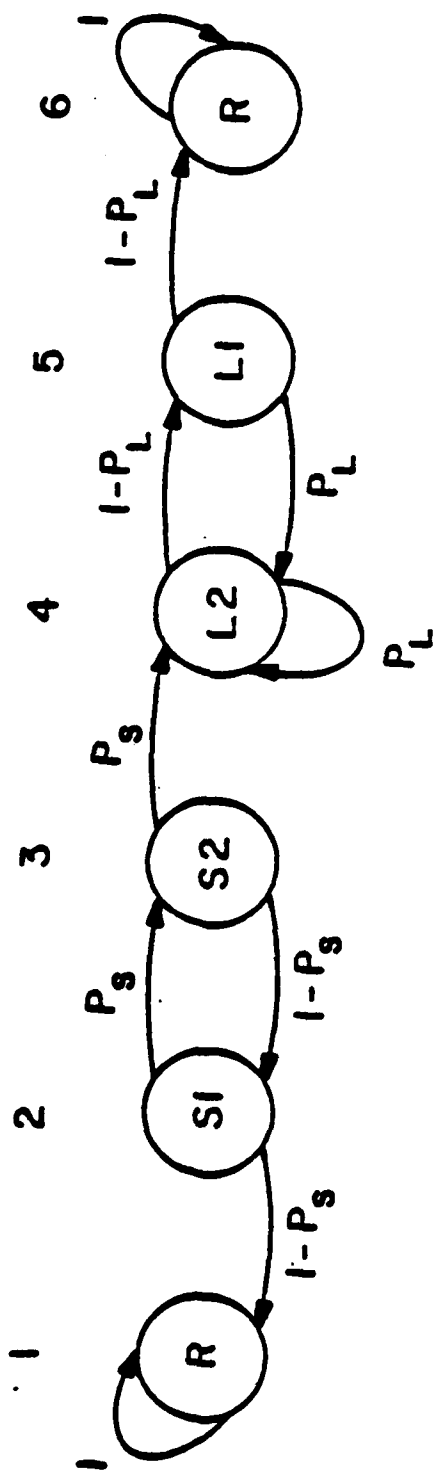

Fig. 2 Markov chain model of search/lock strategy

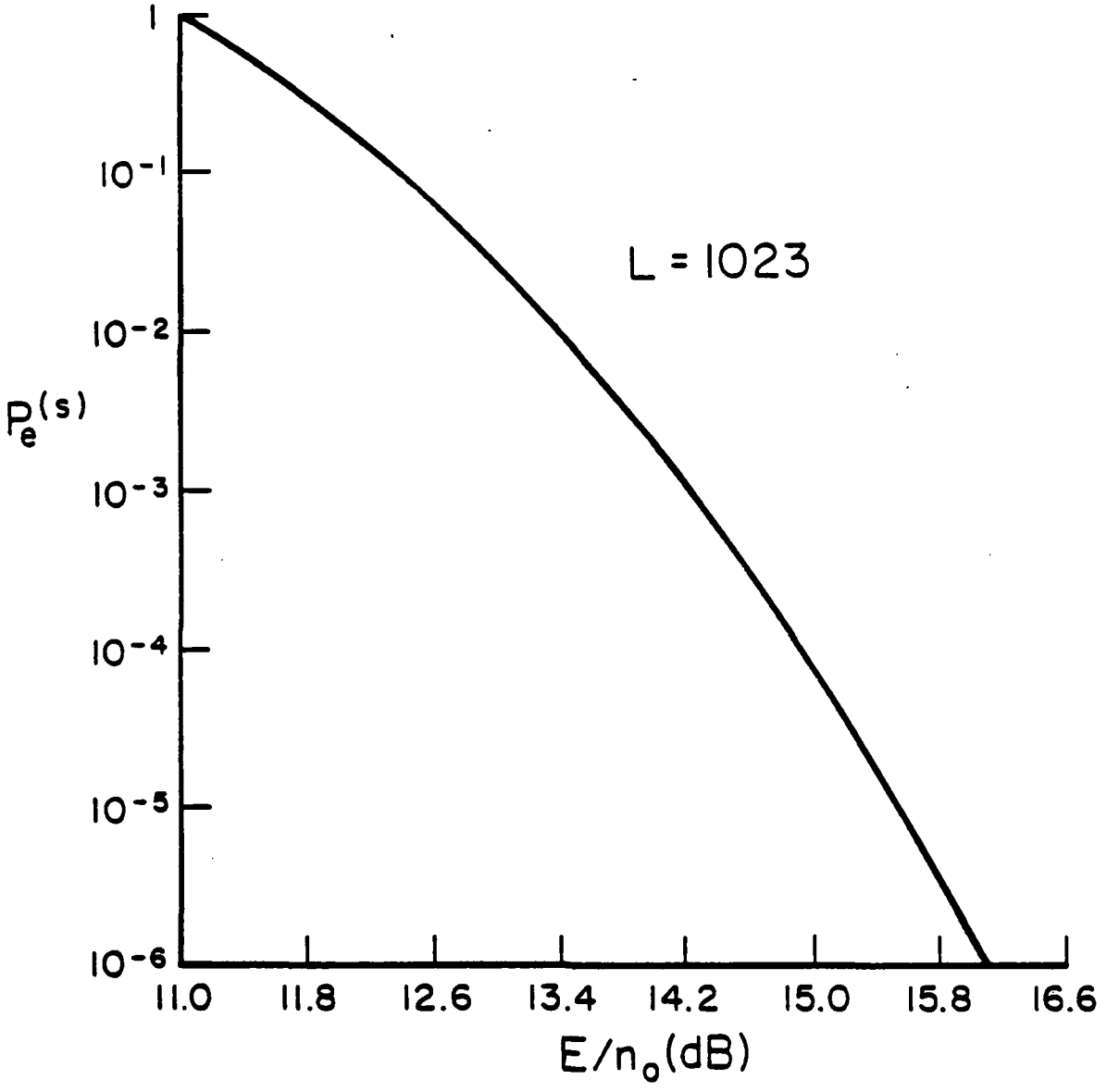

Figure 3. Upper bound on probability of error in the search mode for N = 11 and M = 93.

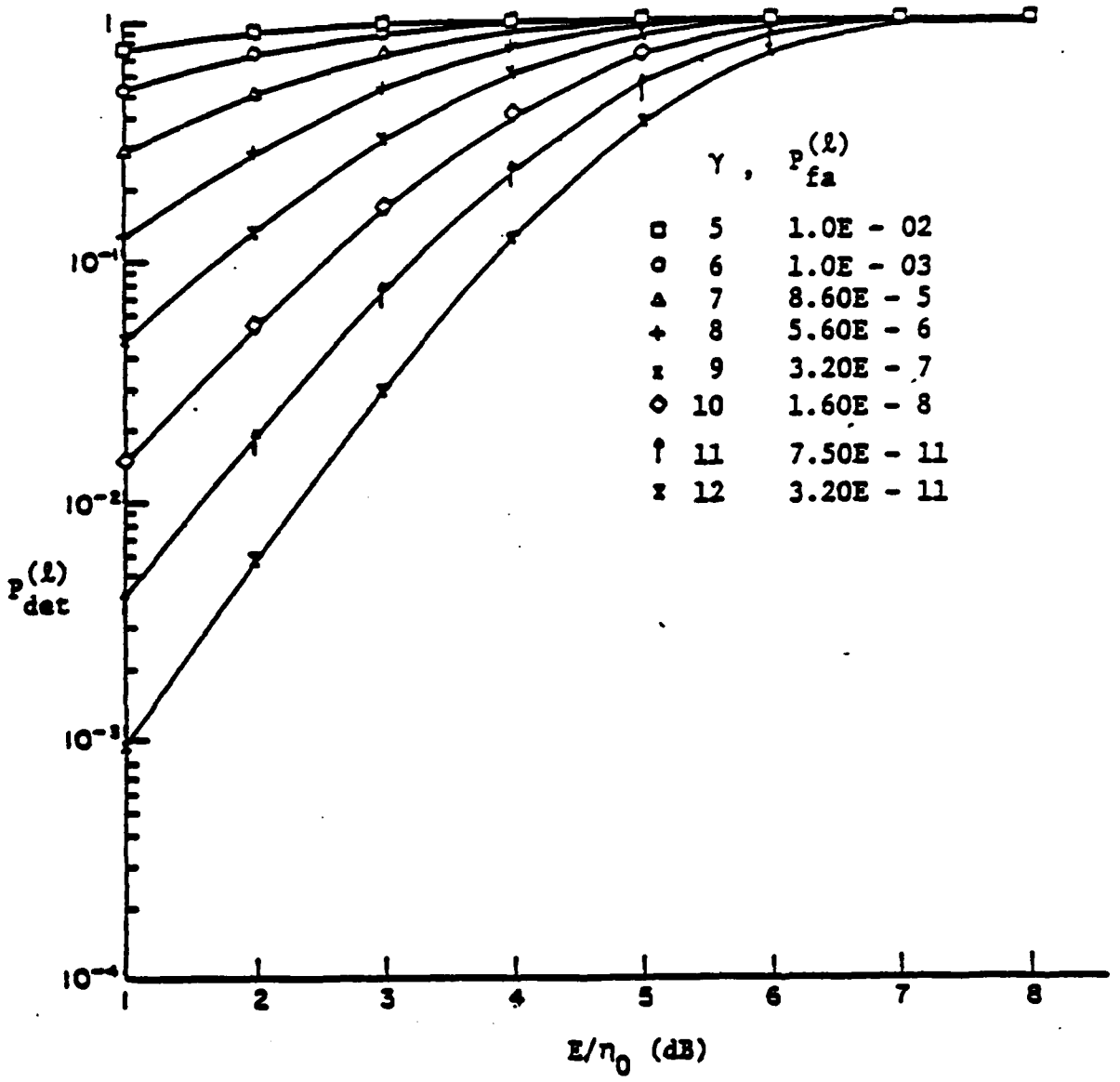

Figure 4 Probability of detection vs E/η_0 for various values of threshold, for N = 11 and M = 93 in the lock mode

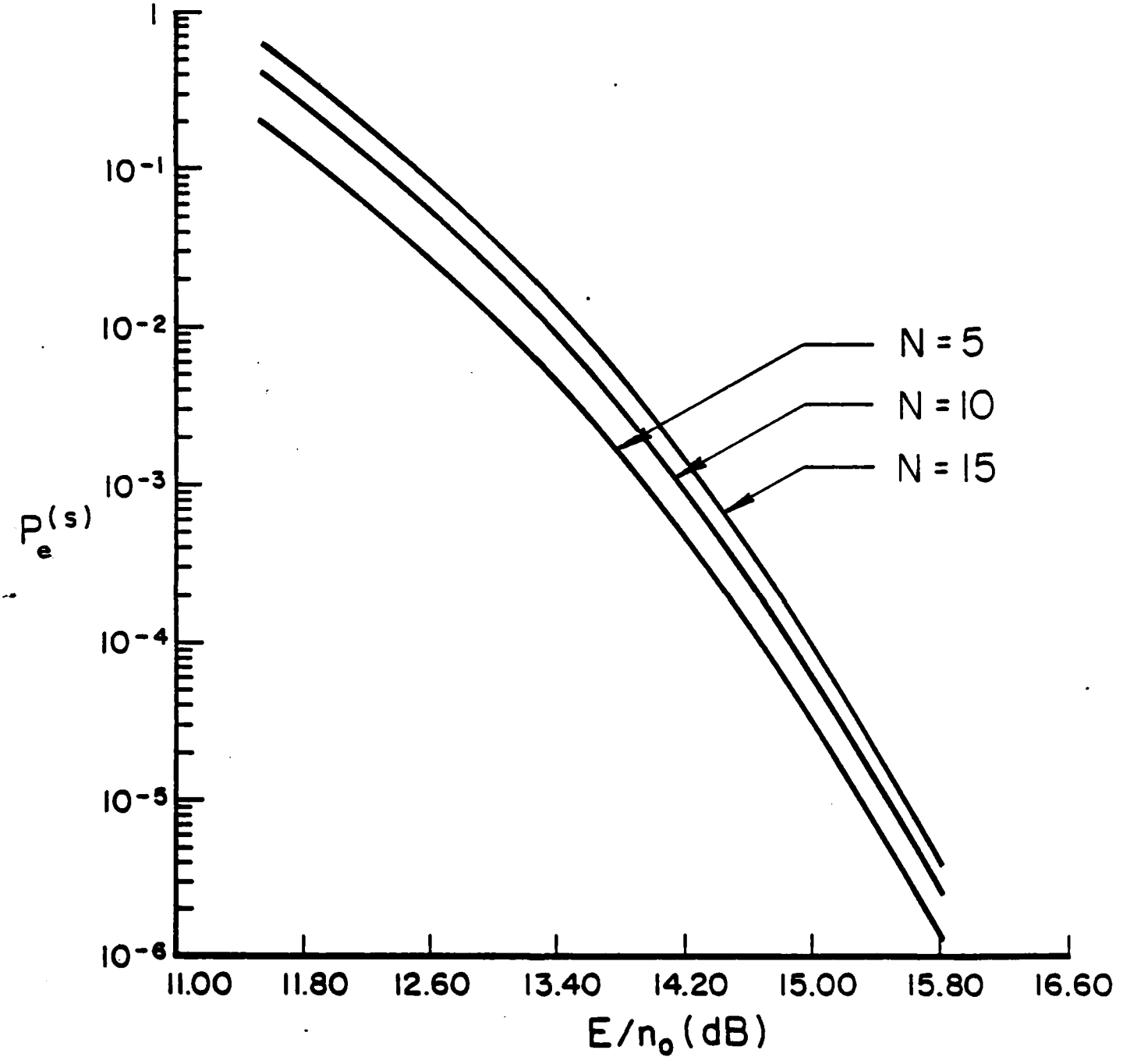

Figure 5. Probability of error in the search mode for various N and M = 93.

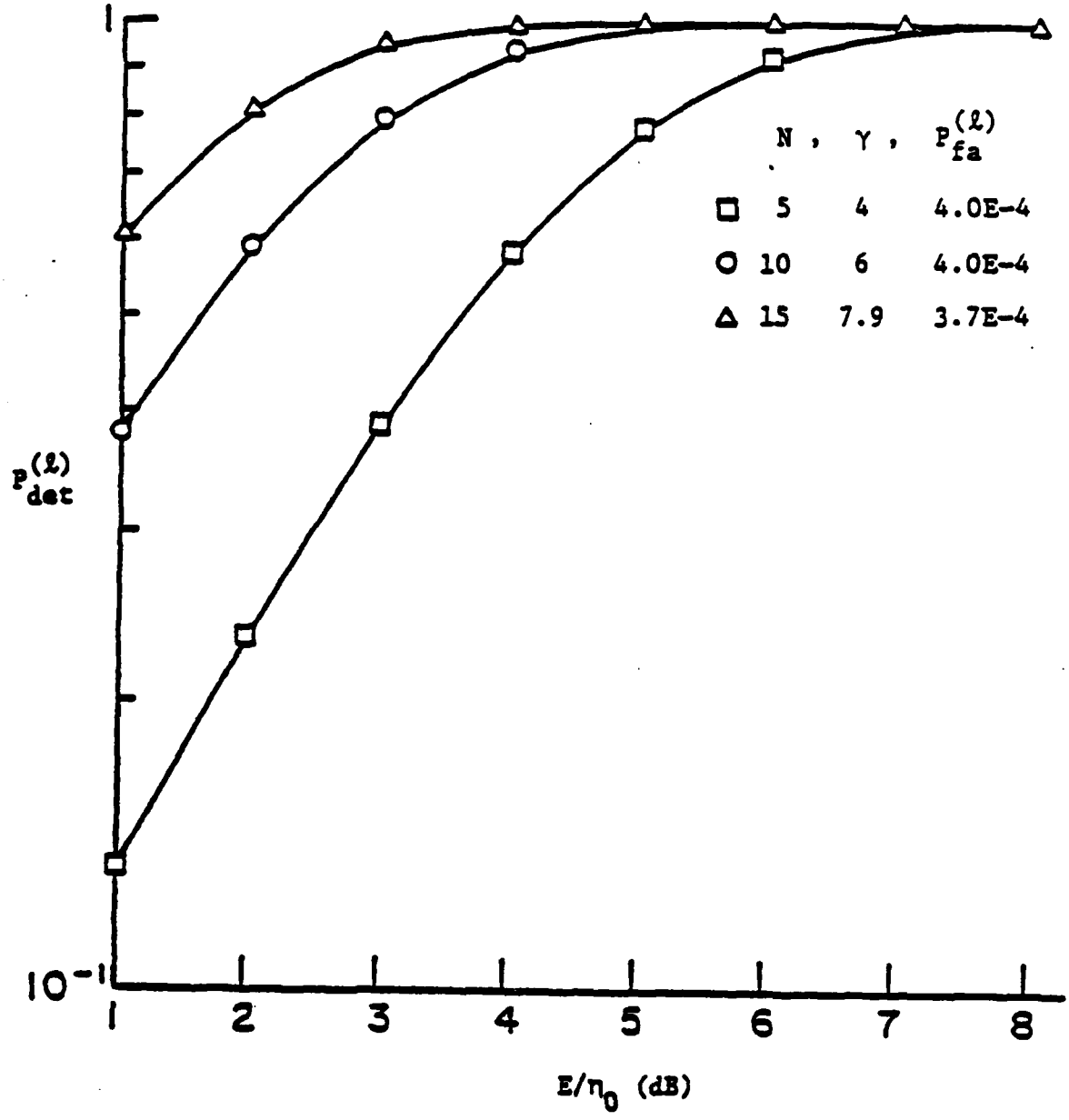

Figure 6 Probability of detection in the lock mode for N = 5, 10, 15

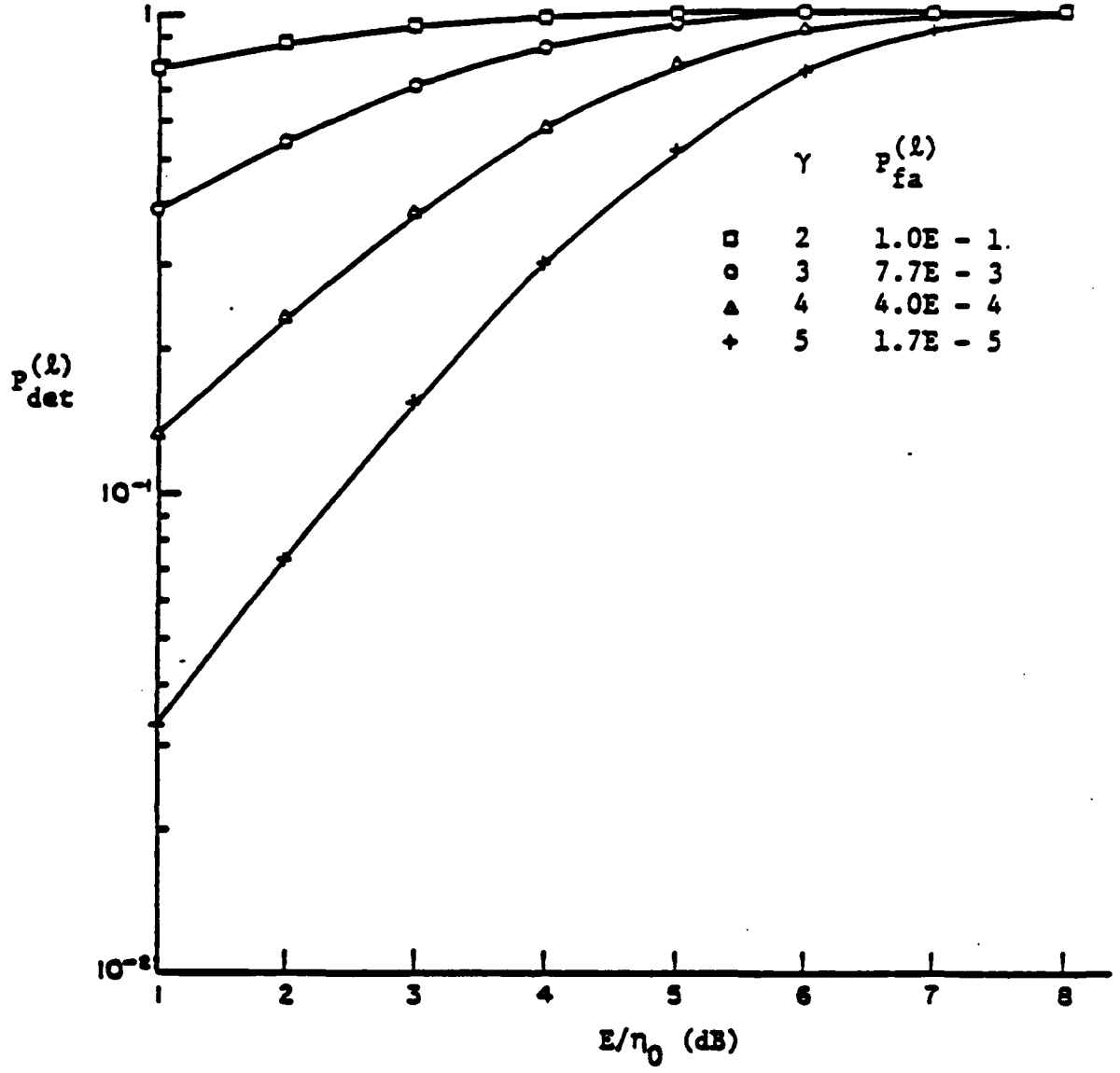

Figure 7 Probability of detection for various thresholds in lock mode (N = 5)

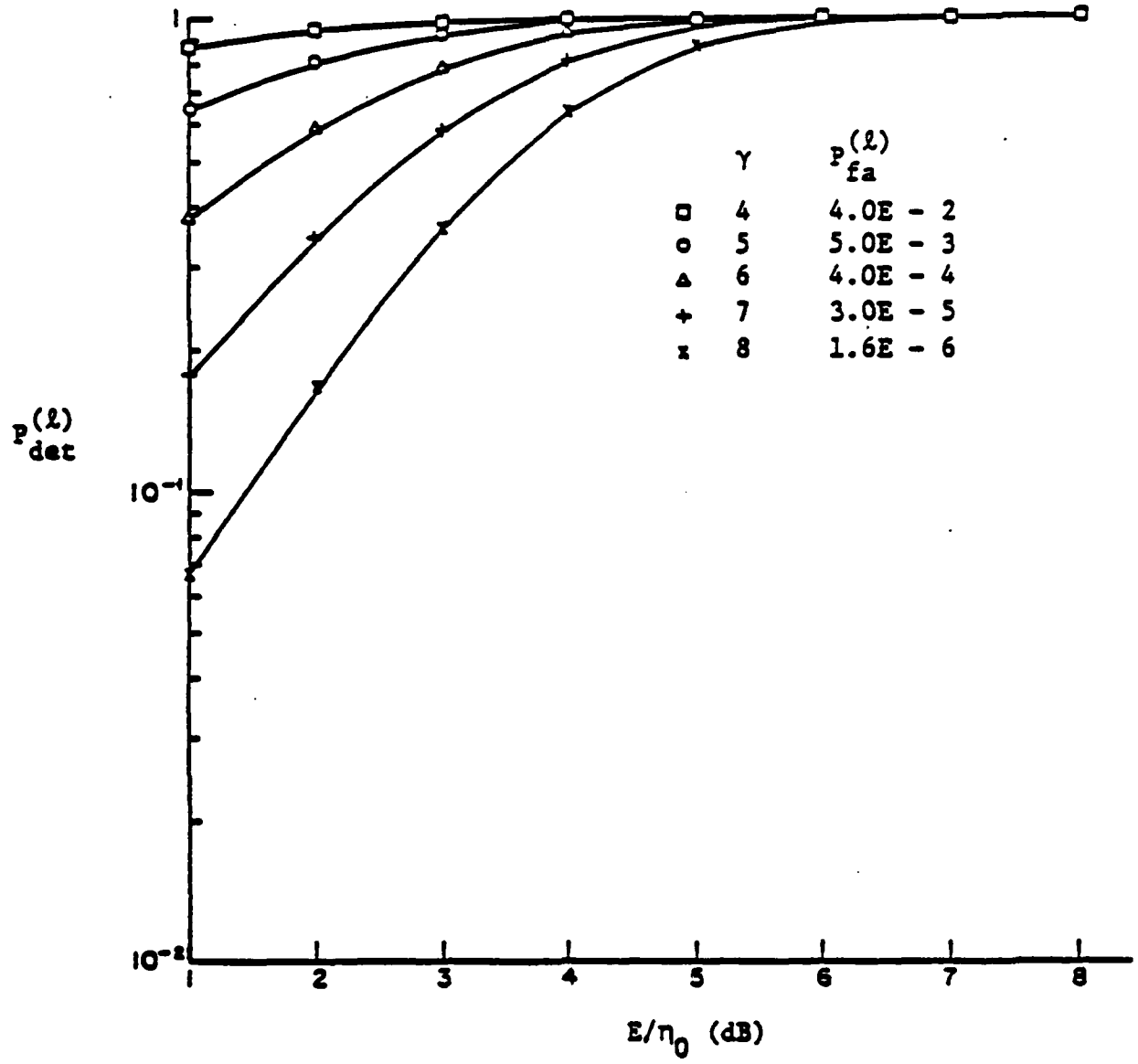

Figure 8 Probability of detection for various thresholds in lock mode (N = 10)

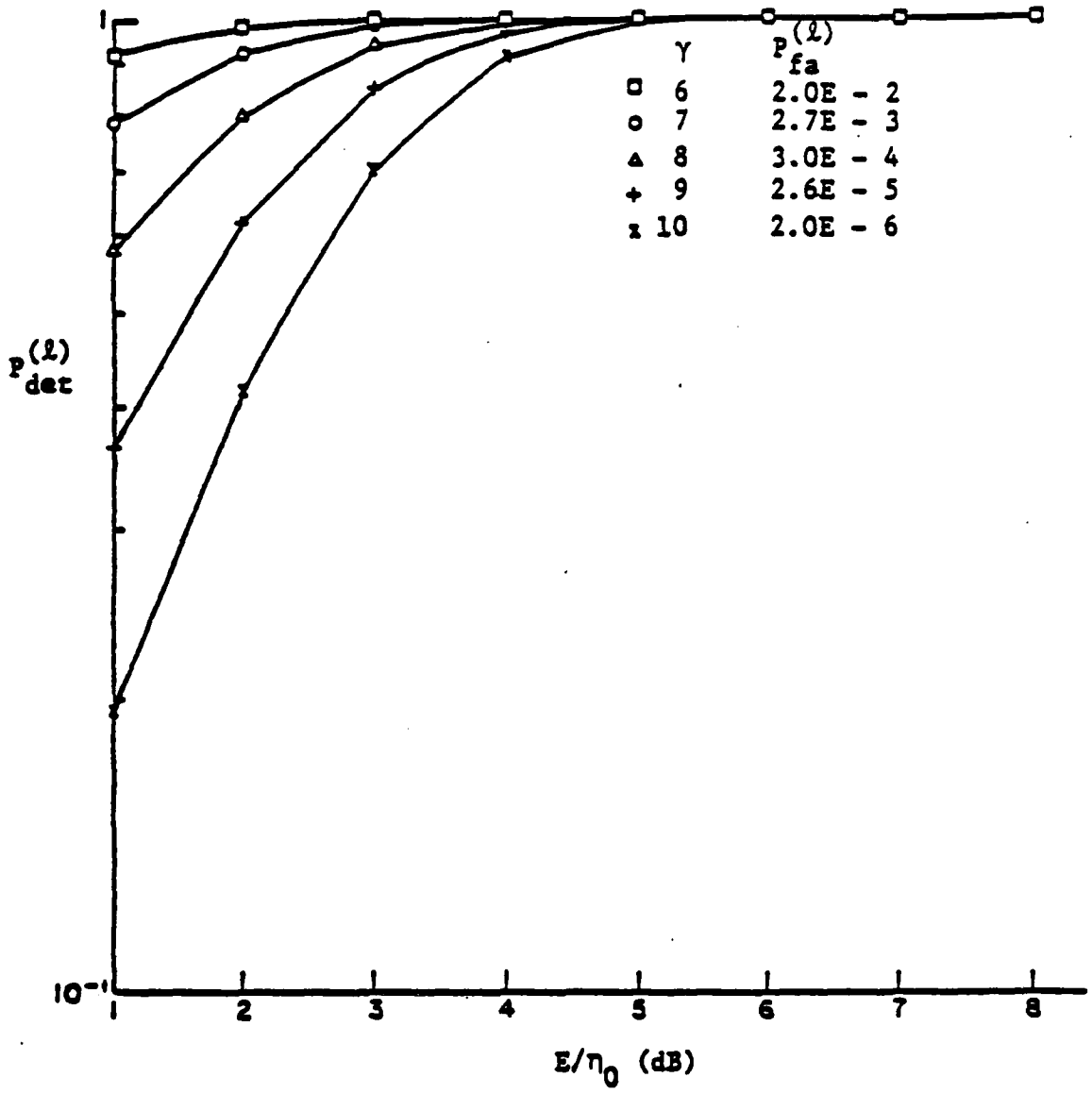

Figure 9 Probability of detection for various thresholds in lock mode (N = 15)

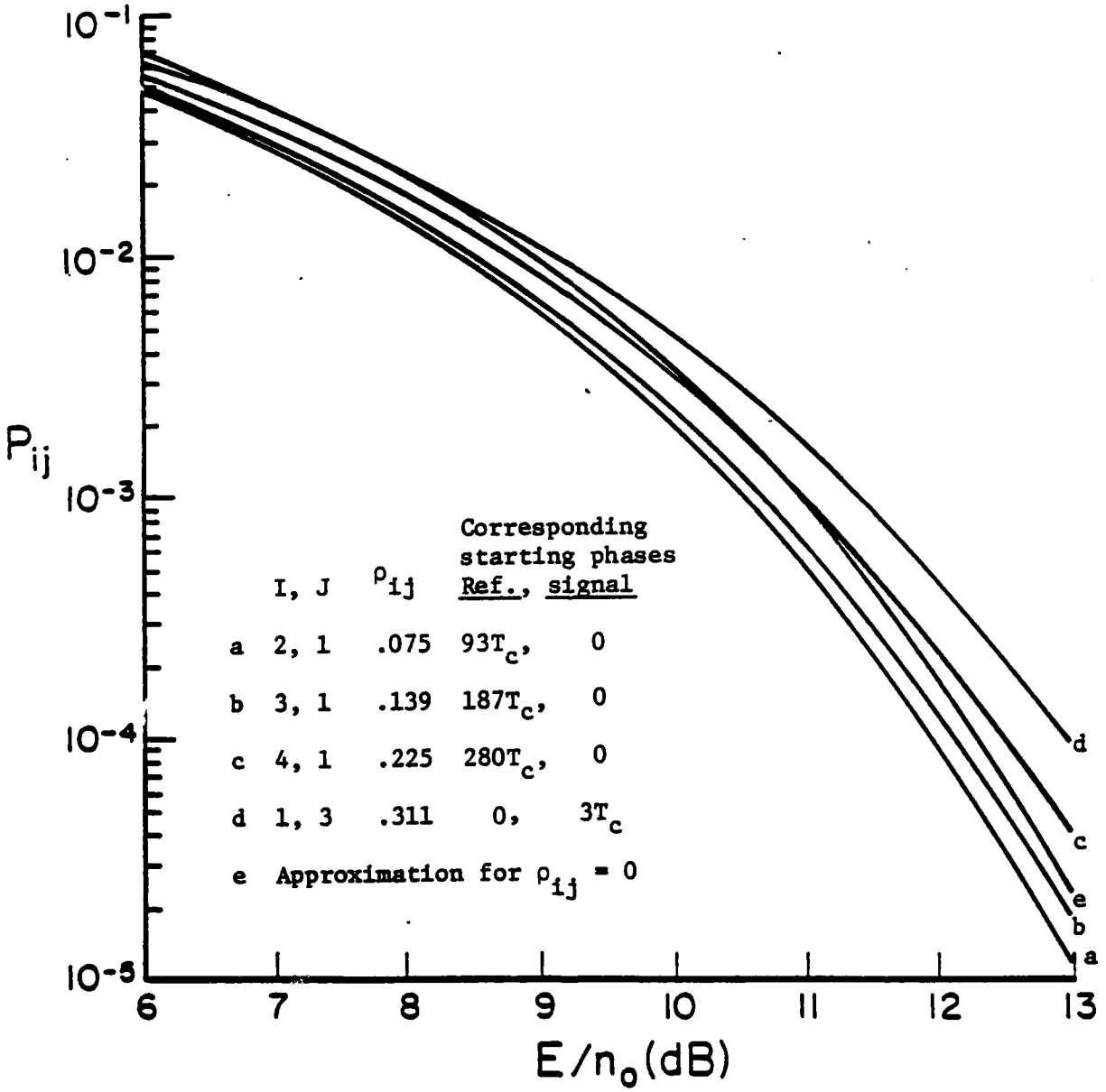

Figure 10. Probability of error for various relative starting phases of reference and input for N = 11 and M = 93 in the search mode.

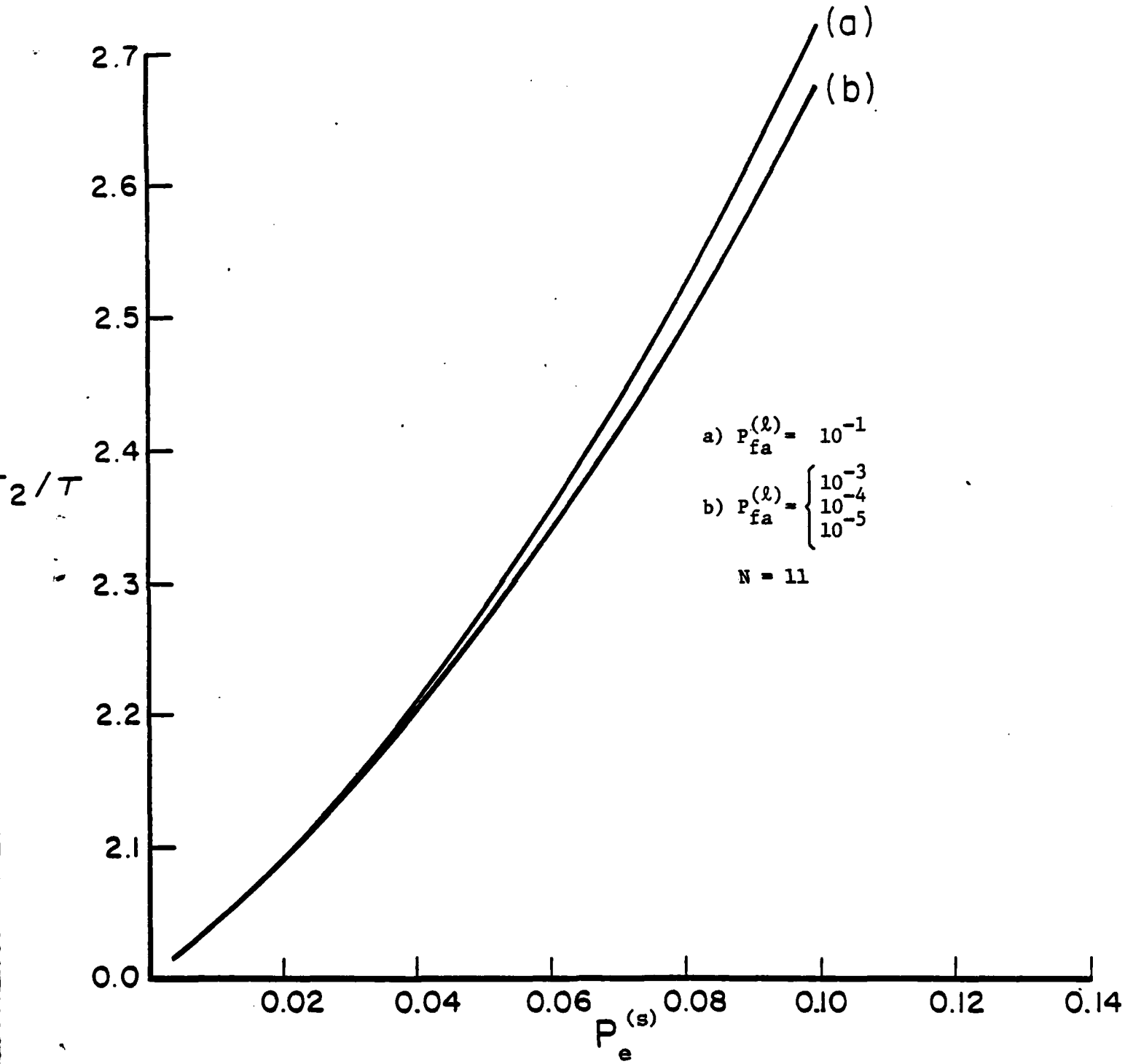

Figure 11. Mean-dwell time versus the false alarm probability in the search mode for various values of the false alarm probability in the lock mode

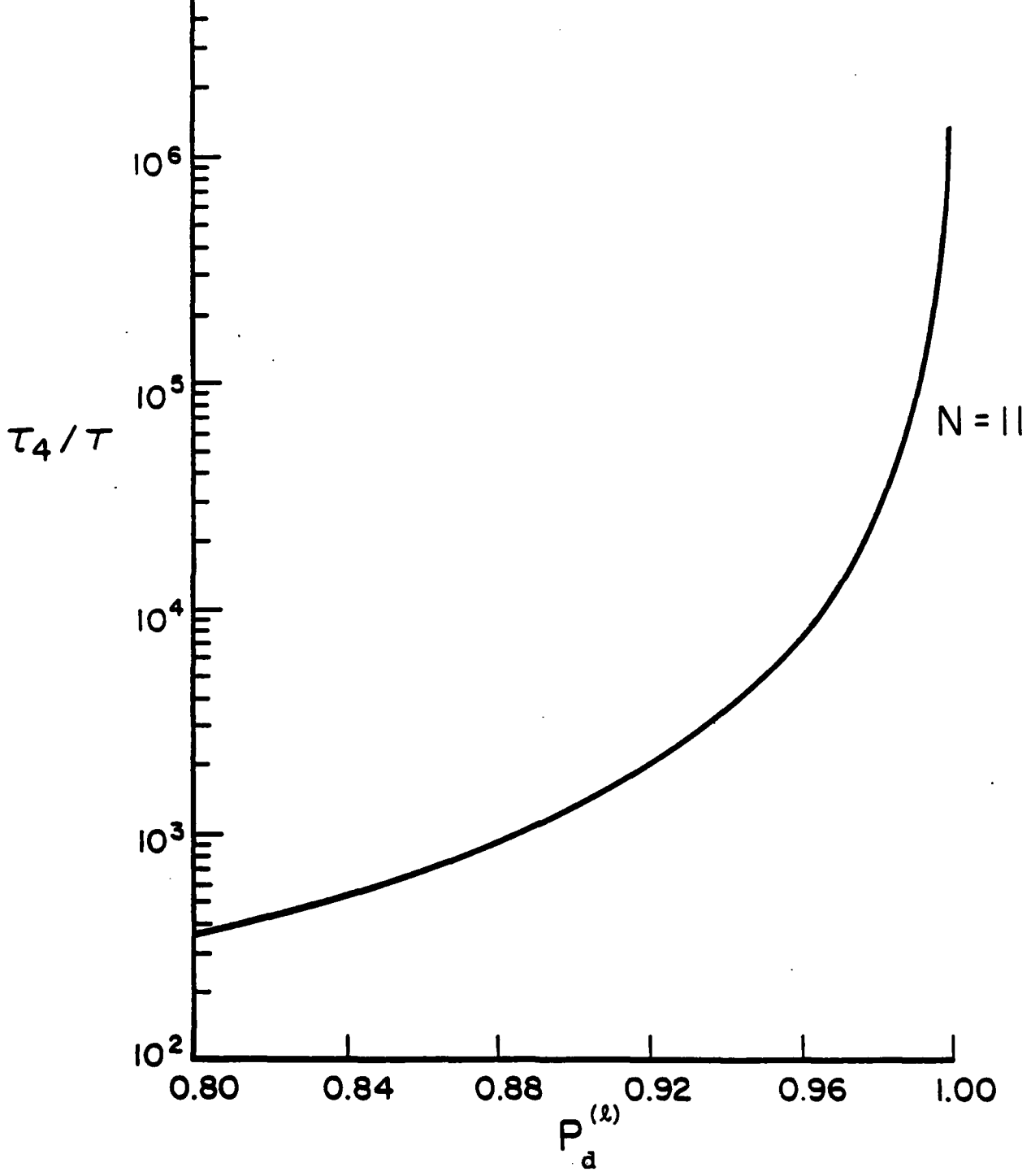

Figure 12. Mean-time to loss-of-lock versus the probability of correct detection in the lock mode.

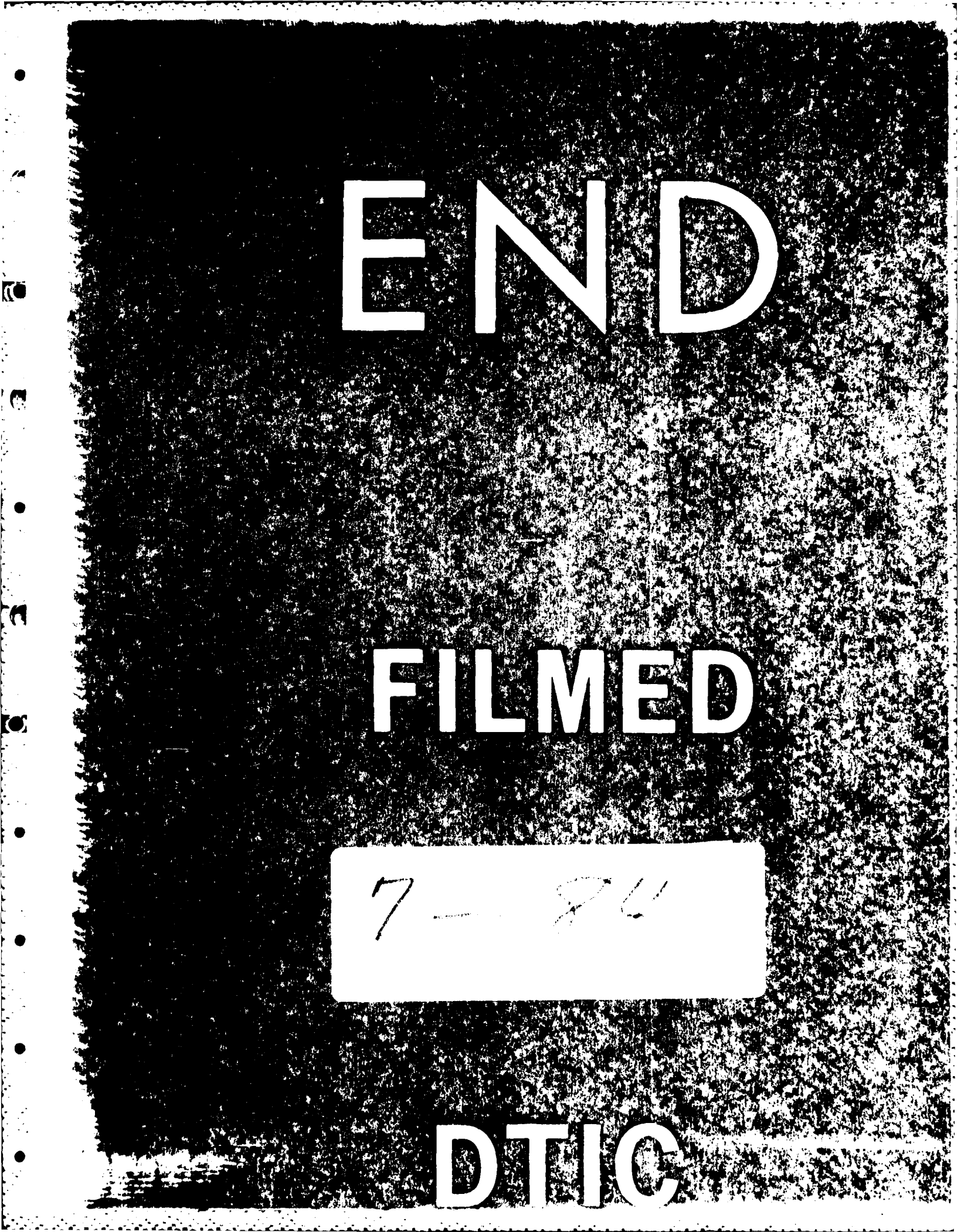
END
FILMED
7-84
DTIC